ACKNOWLEDGEMENTS

I wish to thank my advisor, Richard S. Barr, and my committee members for their patience and support.

I am especially indebted to Tom Tillotson for his leadership and knowledge in the field of digital signal processing as applied to signals intelligence. The previous sentence hardly begins to acknowledge the true technical and personal benefit I've received from knowing Tom. I also want to thank everyone else at Raytheon E-Systems, Greenville Division. I especially want to thank Dennis Close for solving the difficult problems, in the lab. Without his dedication and engineering skill I would not have had time to pursue my education at SMU. I must also mention (in no particular order) Steve Thornton, Brian Holden, Keith Smith, Kevin Spinhirn, Pat Carter, James Miller, John Payne, Jim Pitts, Charlie Blair, John Bishop, Greg Chesney, John Brickman, Mike McBride, David Lacey, Jeff Marquis, Neil Cooper, Mark Bigham, Randy Katz, Earl Wilson, John Brown, Carl Wilson, Wes Redus, Dr. Marvin Eargle, Dr. Fred Curtis, Kevin Cobble, Judd Foss, Greg Loseke, John Hodap, Ryan Robertson, Jeff Meeder, Lisa Bagwill, Mark Kahn, Tom Biedka, Darrel Judd and James McClellen. Thank you for allowing me to have ten years of almost continuous professional and personal growth.

A special thanks to the E-Systems library staff Rogene Ketcham and Linda Moore. I remember the evening Linda returned and opened the library for me so I could do research on this Praxis after hours. Also, thanks goes to Rogene for assisting me in locating the CAIV material that appears in Chapter 7.

To Lavelle Capps and Ethyl Young who taught me when I was a baby and instilled in me a love for learning, laughter and determination. I hope this in some small way repays the prayers you have said for me.

To my Dawn who has been a constant encouragement for the past two years: mi amor.

I extend a special thanks to all of my family, but especially my 10 year old son, Albert, who has sacrificed to complete this work by spending many extra hours by himself without his Dad. Now that its over we are going to have some fun!

And finally no acknowledgment would be complete without mentioning my Dad, Albert Clifton Young, Jr. (his wife Glenda) and my mother Iva Lee Young. They are amazing people and I wouldn't trade them for any other parents in the world.

Young, Darrell Lee B.S., Oklahoma State University, 1983
M.S., Oklahoma State University, 1987

Robust Emitter Location for Application within an Information Fusion Architecture

Advisor: Professor Richard S. Barr

Doctor of Engineering degree conferred May 1997

Praxis completed April 1997

Robust formulations for emitter location are developed for the following three types of emitter location systems: 1) Direction of Arrival (DOA); 2) Time Difference of Arrival (TDOA) and 3) Frequency Difference of Arrival (FDOA). The robustness is achieved by minimizing the mean absolute value of the deviations via linear programming. Update procedures for processing the data in real-time are also described.

The statistical characteristics of DOA, TDOA and FDOA estimators and the circumstances surrounding ambiguous estimates are examined. Ambiguous estimates disrupt the otherwise Gaussian error distribution of the measurements. It is in these cases that the advantage of the robust approach becomes apparent.

Furthermore the robust approach is highly useful when attempting to associate measurements to a single source when multiple sources are present and not easily distinguished. Clustering and partitioning algorithms are discussed. An example that shows the utility of the proposed approach for separating multiple emitters is given.

Finally the linear program is incorporated into a Level 1 fusion architecture which utilizes all three submodels, DOA, TDOA and FDOA, to successfully associate measurements and locate emitters in dense environments.

TABLE OF CONTENTS

LIST OF TABLES

Table Page

LIST OF FIGURES

Figure Page

Chapter 1

Introduction

The advent of automated systems has produced organizational operating environments rich in digital data. On the whole automation has been extremely beneficial in meeting enterprise objectives. However, the sheer amount of information available can be overwhelming and confusing. For example, it has become legendary that when the Air Force first installed automated missile warning systems in the cockpit that pilots sometimes ignored or disabled them under the extreme pressure of the information overload they experienced in difficult combat situations.

Data information fusion is needed to reduce the flow of information to a meaningful, manageable stream. Data information fusion is one of the high leverage technologies necessary for the military to successfully take full advantage of the digital battlefield [AU96, USAF96]. Likewise, enterprise-wide coordination and information sharing has been the focus of commercial endeavors. Techniques to associate, reduce and give meaning to the large amount of data available to the modern organization have included neural networks, fuzzy logic and various forms of expert systems. A successful information fusion system may encompass these multiple methods at various levels so that they become complementary. In this vein it is no surprise that mathematical programming techniques also appear. Mathematical programming (linear and integer

programming) and its practitioners have historically been involved in the development of decision support systems for both government and industrial applications.

One aspect of the battlefield information fusion problem consists of associating measurements made from various sensors in order to locate and track emitters. Emitters may be either electromagnetic or acoustic. Examples of radio emissions are Morse code transmissions, voice, data links, radars and beacons. Acoustic energy is of primary interest to naval operations where SONAR is used to locate and track ships and submarines. The primary location measurements are Direction of Arrival (DOA), Time Difference of Arrival (TDOA) and Frequency Difference of Arrival (FDOA). Additional signal measurements such as fine frequency and modulation format may be useful in associating the primary measurements with the emitter sites from which they originate.

In a dense environment it can be difficult to correctly separate measured parameters into groups (emitter files) for location estimation because it may not be clear if the measurement belongs with an existing estimated location or if it should be used to begin a new emitter file. In the past difficult decisions of this sort, which involve associating parameter measurements to emitter sites to obtain a refined location estimate, has been a manual process. However, the capability of new sensor systems to rapidly measure and generate voluminous amounts of parameter data (i.e. DOA, TDOA, FDOA, etc.) completely outpaces the analytical manpower available. New automated methods are needed to reliably perform the association without human assistance.

The unique benefit of the linear programming approach for emitter location as proposed in Chapter 2 is its ability to minimize the sum of *absolute* deviations versus the

more common method which minimizes the sum of *squared* deviations (also termed the least squares approach). The increased location accuracy of minimizing the absolute deviations enables quick partitioning algorithms to correctly associate the measurements with emitters. A specific numerical example will be given later but the difference between the two approaches has been portrayed as follows.

Envision a heat seeking missile approaching a target aircraft which has deployed a hot decoy countermeasure. The missile seeker algorithm is faced with a choice. On the one hand minimization of the squared deviations between the target and the decoy results in the missile "splitting the difference" and hitting neither the target nor the decoy but instead passing between the two. In effect the least squares approach assures a miss when two targets are present because the route between the targets minimizes the least squares cost function. On the other hand the proposed linear programming approach minimizes the absolute deviations which results in a missile trajectory that pursues either the aircraft *or* the decoy.

The fifty-fifty chance of pursuing the right target is infinitely better than the guaranteed failure of the least squares approach. However, additional processing can significantly improve the odds. In particular the deviations can be treated as an output of the linear program and combined with other available measurements such as thermal characteristics and scene features. The clustering of measurements will identify an aircraft set and a decoy set. Then performing separate least squares analysis of these two sets may now be appropriate to yield optimum (and separate) location estimates of the target and the decoy.

As will be shown the least squares estimator is optimum only when the deviations are normally distributed. While minimization of the squared deviations may be appropriate once the measurements have been separated into groups, prior to separation the least squares approach is inadequate. This suggests a multi-stage fusion architecture where the first stage is concerned with obtaining initial estimates of emitter locations, the second stage performs grouping of the measurements and finally the last stage operates on the sets of grouped data to yield precision location estimates of the multiple emitters in the environment. Such an architecture is presented in Chapter 6.

The usefulness of the mathematical programming approach is evident when multiple targets are present because of its tendency to make an either-or decision. However, it can also be useful when only a single target is in the environment because of the unfortunate tendency of DOA, TDOA and FDOA estimators to occasionally report ambiguous results. These false reports can have the same deleterious effect as the decoy in the above example.

The statistical characteristics of DOA, TDOA and FDOA estimators and the circumstances surrounding ambiguous estimates are examined in Chapter 2. In Chapter 3 a linear program is formulated for DOA, TDOA and FDOA emitter location. Update procedures for processing the data in real-time as it arrives are described in Chapter 4. Chapter 5 describes clustering algorithms and gives an example that shows the utility of the proposed approach for separating multiple emitters. Chapter 6 performs Monte Carlo testing and comparison of all the algorithms and also describes how the linear program can be incorporated into a fusion architecture to successfully associate measurements and locate emitters. Finally, Chapter 7 develops an economic model that performs algorithm

selection and system sizing to maximize profit while simultaneously minimizing risk and meeting cost and performance objectives.

Chapter 2

Statistics of Location Parameter Measurements

The proposed linear programming approach for emitter location is superior when measurements from multiple emitters are inadvertently mixed together causing a cross contamination in the estimation process or when ambiguities due to the measurement process cause outliers in the estimated DOA, TDOA or FDOA location parameters. Nearby emitters cause cross contamination when the location parameter is measured to a first signal and then shortly after it has stopped transmitting a second nearby signal begins transmitting. Because of measurement noise it is not always clear that the two location parameter estimates should be kept separate. It is ironic that the cochannel signal problem, which is considered more difficult because two or more signals are simultaneously interfering with each other, is actually less difficult in the respect that if two different signals are simultaneously detected in the location parameter space then their location parameters can be unambiguously assigned to different emitter files. For example, the multiplatform signal processing approach proposed by Agee and Young [AY90] allows sorting of cochannels signals based on their TDOA or FDOA parameters whereas if the signals appear separated in time then deciding if they originated from the same location can be difficult.

Ambiguities in the measurement process in either the single signal case or in cochannel can cause substantial degradation of accuracy unless removed or processed in

some robust manner. Kriel and Yarlagada [KY88, Kri88] have shown improved DOA estimation performance (relative to least squares) by using an L_p norm (with $p<2$) for spatial spectral processing when the array noise contained outliers.

Ambiguities in the DOA measurement process occurs because of competing minima in the DOA cost function. DOA processing consists of comparing a measured array response to a collection of prestored responses that are indexed by DOA. An array response is a vector of sensor phases and magnitudes measured with respect to some reference (usually one of the sensors). Type I ambiguities occur in the measurement of DOA when a single signal arriving from direction θ_1 causes an array response that is nearly identical to an array response from a second direction θ_2. Type II ambiguities can exist when two signals are present [Sch79]. A strong ambiguity at θ_2 means that the DOA measurement process is just as likely to report θ_2 as θ_1 even when noise levels are low. On the other hand a weak ambiguity is usually not a problem when the noise level is low because the system has discrimination margin. However, as noise levels increase so does the ambiguity rate. The ambiguity rate is the fraction of ambiguous reports relative to the total.

TDOA measurements can also suffer from ambiguities. The two main types of TDOA systems are those which measure pulse events and those that perform cross correlation on continuous signals. Both are susceptible to ambiguities. For a transmitter emitting a series of pulses received by multiple stations the potential ambiguity arises when the time difference between stations exceeds the time between successive pulse transmissions. Time delay between continuous signals is estimated by locating the peak

of the cross-correlation function. Cross correlation functions can have multiple competing maxima. Narrowband signals are especially prone to exhibit peaks adjacent to global peak. In the presence of noise and finite observation times the side peaks are occasionally picked as the dominate peak [CS81]. The probability of ambiguous peaks is derived in [MS84]. This effect can degrade the performance of TDOA systems.

FDOA measurements are not immune to ambiguities. For example, the multiple harmonics in a standard broadcast television signal can cause competing minima in an FDOA cost function. Although FDOA correlation takes place in the frequency domain it otherwise has similar properties as TDOA estimators in that it is subject to the deleterious effects of ambiguous peaks that result when processing certain signal structures.

When ambiguities are absent, location parameter estimates (DOA, TDOA and FDOA) can generally be assumed to be Gaussian. However, when ambiguities are present the resulting distribution is decidedly non-Gaussian. The process is illustrated in figure 1.

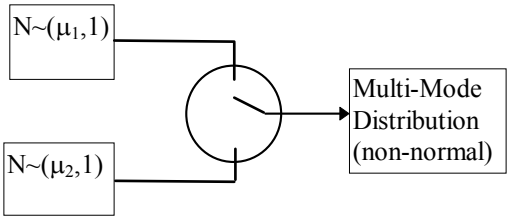

Figure 1 Nonlinear Combination of Two Normal Processes Yields a Non-Normal.

Suppose that the top block represents the true measurements when ambiguities are absent. Give it mean μ_1 and unity variance. Let the bottom block represent the ambiguity. Let the distribution of the ambiguity be normal with unity variance but with a

different mean μ_2. The ambiguity rate is the fraction of time the switch is in the bottom position. The resulting mixed probability density function is

$$p(x) = {}^{1}\!/_{\sqrt{2\pi}}\left((1-\alpha)\int e^{(x-\mu_1)^2}\,dx + \alpha\int e^{(x-\mu 2)^2}\,dx\right). \quad (1)$$

Where α is the ambiguity rate. Equation 1 can be easily extended when multiple ambiguities are present with different variances. The following equation describes the probability distribution function when two ambiguities are present:

$$p(x) = {}^{1}\!/_{\sqrt{\pi}}\left(\frac{\alpha_1}{\sigma_1}\int e^{\frac{(x-\mu_1)^2}{\sigma_1^2}}\,dx + \frac{\left(1-\alpha_1-\alpha_2\right)}{\sigma_0}\int e^{\frac{(x-\mu_0)^2}{\sigma_0^2}}\,dx + \frac{\alpha_2}{\sigma_2}\int e^{\frac{(x-\mu_2)^2}{\sigma_2^2}}\,dx\right). \quad (2)$$

Equation 2 is used in the robust fusion model presented in Chapter 6 to generate the measurement noise for DOA, TDOA and FDOA observations.

Ekblom and Henriksson [EH69] have shown that L_p with $p<2$ performs better than least squares (which is L_2) for estimating the mean of mixed exponential and rectangular distributions. Minimizing the sum of absolute deviations is L_1. Their results implies that L_1 processing may be more appropriate than least squares anytime the data is "almost clean":

> By "almost clean" we mean that a certain proportion of the data comes from the distribution whose location parameter we intend to study, but that some of the data consists of "outliers." This of course means that we have a mixed distribution with one part coming from a perturbing distribution [EH69].

If the difference between the mean arising from the ambiguity and the true mean is large enough then a prefiltering operation may be sufficient to remove the outliers. However, in many cases the ambiguity is too near to the true mean to be immediately rejected. This

is particularly true when the number of prior observations is low because the estimated variance is still high and cannot be used to discriminate nearby ambiguities.

The advantage of the L_1 approach to emitter location is that it allows the screening process to proceed after an initial location has been computed. The linear program effectively ignores outliers and yields a good location estimate which can be used to initiate a grouping of measurements for subsequent ambiguity-free location refinement.

Chapter 3

Emitter Location Algorithms

The approach for each model, DOA, TDOA and FDOA, is to derive the linearized least squares solution and then use the linearized equations to formulate a linear program to minimize the sum of absolute deviations.

3.1 Emitter Location From Bearing Data

Obtaining emitter location from bearing data has been of interest for some time. Triangulation problems occur in geodetic surveying networks, in submarine location by sonar, in parallax determination in astronomy, and so forth [Taf97]. One of the first papers on this subject was published by d'Ocagne [d1893]. The problem he posed was to minimize the sum of the weighted squared distances from a point to a collection of lines. During World War II there was considerable interest in the problem of cross-fixing a target by intercepting radio transmissions and determining their directions relative to a distributed set of receivers [Sta47]. In the following, the problem is first described and then in 3.1.1 the linearized least squares solution is presented. The linearization gives a basis on which a linear program can be formulated which minimizes the absolute value of the deviations versus their squares. The linear program formulation is presented in 3.1.2.

A series of north relative bearing measurements, β_1, β_2, ...β_N, are made from various station points with the goal of intersecting the resulting Lines-of-Bearings (LOBs) to determine a geolocation of an emitter of interest. The station coordinates are

represented in a two-dimensional plane by (x_1,y_1), (x_2,y_2), ... (x_N,y_N). Transformation of latitude and longitude into the x-y plane is accomplished by projecting an earth centered radius through each of the station's latitude, longitude and altitude coordinates into the x-y plane. The x-y plane is tangent to the earth's surface at a nearby but arbitrarily selected stay-point. Two-dimensional algorithms are applied to the transformed measurements to estimate the emitter location. The estimated emitter location is then transformed back into latitude and longitude by finding the intersection of an earth centered radius with the earth's surface and the estimated location in the x-y plane.

The bearing measurement error is given by,

$$e_i = \theta_i - \tan^{-1}\left(\frac{y_T - y_i}{x_T - x_i}\right) \qquad i = 1,\ldots,N \tag{3}$$

where (x_T,y_T) are the true coordinates of the location we desire to estimate. The north relative bearing angle is related to the angle measured counter-clockwise from the x-axis by $\theta_i = \pi/2 - \beta_i$. N_D is the number of bearing measurements. In matrix form (3) can be written as,

$$\mathbf{e} = \boldsymbol{\theta} - \mathbf{f}(\mathbf{q}) \tag{4}$$

where $\mathbf{e}$, $\boldsymbol{\theta}$ and $\mathbf{f}(\mathbf{q})$ are N-dimensional column vectors. The operator $\mathbf{f}$ represents the non-linear inverse tangent function and $\mathbf{q}$ is an N length column vector of arguments which contain the location parameters, x_T and y_T as parameters.

3.1.1 Least Squares Method - Bearing Data

Figure 2 illustrates the non-linear problem of locating an emitter from a collection of N_D noisy bearing estimates.

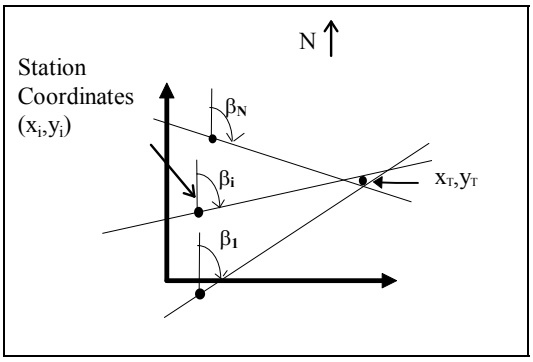

Figure 2 Illustration of Bearing-Only Emitter Location

The derivation of linearized least squares location estimators and their accuracy has been described by Torrieri [Tor84]. The error is assumed to be a multivariate random vector with an N_DxN_D positive-definite covariance matrix

$$\mathbf{S}=\mathrm{E}\{(\mathbf{e}-\mathrm{E}\{\mathbf{e}\})(\mathbf{e}-\mathrm{E}\{\mathbf{e}\})^{\mathrm{T}}\}, \tag{5}$$

where E{ } denotes the expected value and the superscript T denotes the transpose. If **e** is assumed to have a zero mean and a Gaussian distribution, then the conditional density function of $\boldsymbol{\theta}$ given **q** is

$$p(\boldsymbol{\theta}|\mathbf{q})=\frac{\mathbf{1}}{(\mathbf{2}\pi)^{N/2}|\mathbf{S}|^{1/2}}\exp\{-(1/2)[\boldsymbol{\theta}-\mathbf{f}(\mathbf{q})]^{\mathrm{T}}\mathbf{S}^{-1}[\boldsymbol{\theta}-\mathbf{f}(\mathbf{q})]\}. \tag{6}$$

The maximum likelihood estimator is that value of **q** which maximizes the conditional density function. Thus, the maximum likelihood estimator minimizes the quadratic form

$$Z(\mathbf{q})=[\boldsymbol{\theta}-\mathbf{f}(\mathbf{q})]^{\mathrm{T}}\mathbf{S}^{-1}[\boldsymbol{\theta}-\mathbf{f}(\mathbf{q})]. \tag{7}$$

If **f**(**q**) is linear Z(**q**) can be minimized by taking derivatives with respect to the parameters in **q** and solving the resulting system of simultaneous equations. However,

when **f**(**q**) is non-linear, as it is in this case, an estimator can be obtained by expanding **f**(**q**) in a Taylor series about a reference point $\mathbf{q}_o$ and retaining the first two terms,

$$\mathbf{f}(\mathbf{q}) \cong \mathbf{f}(\mathbf{q}_o) + \mathbf{G}(\mathbf{q} - \mathbf{q}_o), \tag{8}$$

where **G** is the Nx2 matrix of derivatives evaluated at $\mathbf{x}_o$,

$$\mathbf{G} = \begin{bmatrix} \frac{\delta f_1}{\delta q_1}\Big|_{\mathbf{q}=\mathbf{q}_o} & \frac{\delta f_2}{\delta q_2}\Big|_{\mathbf{q}=\mathbf{q}_o} \\ \cdot & \cdot \\ \cdot & \cdot \\ \cdot & \cdot \\ \frac{\delta f_N}{\delta q_1}\Big|_{\mathbf{q}=\mathbf{q}_o} & \frac{\delta f_N}{\delta q_2}\Big|_{\mathbf{q}=\mathbf{q}_o} \end{bmatrix}. \tag{9}$$

Let ϕ_{oi} denote the angle from station *i* to the reference point as shown in Figure 3.

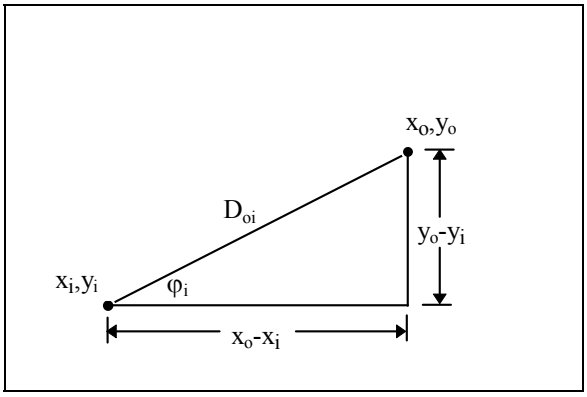

Figure 3 Relationship of Station Coordinates to Reference Point.

Then

$$\sin(\phi_{oi}) = \left(\frac{(y_o - y_i)}{D_{oi}} \right) ; \tag{10}$$

$$\cos(\phi_{oi}) = \left(\frac{(x_o - x_i)}{D_{oi}} \right), \tag{11}$$

where

$$D_{oi} = [(x_o - x_i)^2 + (y_o - y_i)^2]^{1/2} \tag{12}$$

$$\mathrm{i} = 1,2,\ldots,\mathrm{N_D}.$$

The derivative of the inverse tangent function with respect to x is

$$\frac{d(\tan^{-1}\left(y - y_i \big/ x - x_i\right)}{dx} = \frac{-(y - y_i)}{(x - x_i)^2 + (y - y_i)^2}, \tag{13}$$

with respect to y

$$\frac{d(\tan^{-1}\left(y - y_i \big/ x - x_i\right)}{dy} = \frac{(x - x_i)}{(x - x_i)^2 + (y - y_i)^2} \tag{14}$$

so that **G** for the DOA problem can be written as,

$$\mathbf{G}^{\mathrm{DOA}}_{\mathrm{N_D x 2}} = \begin{bmatrix} \frac{-\sin(\phi_{o1})}{\mathrm{D_{o1}}} & \frac{\cos(\phi_{o1})}{\mathrm{D_{o1}}} \\ . & . \\ . & . \\ . & . \\ \frac{-\sin(\phi_{oN})}{\mathrm{D_{oN_D}}} & \frac{\cos(\phi_{oN})}{\mathrm{D_{oN_D}}} \end{bmatrix}. \tag{15}$$

Combining (7) and (8) gives

$$Z^*(\mathbf{q}) = \left[\theta - \left[\mathbf{f}(\mathbf{q_o}) + (\mathbf{G}\left(\mathbf{q} - \mathbf{q_o}\right)\right]\right]^T \mathbf{S}^{-1}\left[\theta - \left[\mathbf{f}(\mathbf{q_o}) + (\mathbf{G}\left(\mathbf{q} - \mathbf{q_o}\right)\right]\right] \tag{16}$$

or,

$$Z^*(\mathbf{q}) = [\theta^* - \mathbf{G}\mathbf{q})]^T \mathbf{S}^{-1}[\theta^* - \mathbf{G}\mathbf{q}] \tag{17}$$

where

$$\theta^* = \theta - \mathbf{f}(\mathbf{q}_o) + \mathbf{G}\mathbf{q}_o. \tag{18}$$

To solve for the parameter estimates $\hat{\mathbf{q}}$ that minimizes $Z^*(\mathbf{q})$ we take the derivatives with respect to the parameters and set the result equal to zero and solve for $\hat{\mathbf{q}}$,

$$2\mathbf{G}^{\mathrm{T}}\mathbf{S}^{-1}\mathbf{G}\hat{\mathbf{q}} - 2\mathbf{G}^{\mathrm{T}}\mathbf{S}^{-1}\boldsymbol{\theta}^{*} = \mathbf{0}. \tag{19}$$

Thus, the solution of (19) is

$$\hat{\mathbf{q}} = (\mathbf{G}^{T}\mathbf{S}^{-1}\mathbf{G})^{-1}\mathbf{G}^{T}\mathbf{S}^{-1}\boldsymbol{\theta}^{*}. \tag{20}$$

Replacing θ^* with $[\theta - f(q_o)+Gq_o]$ gives the linearized least squares estimator,

$$\hat{\mathbf{q}} = \mathbf{q}_{o} + (\mathbf{G}^{T}\mathbf{S}^{-1}\mathbf{G})^{-1}\mathbf{G}^{T}\mathbf{S}^{-1}[\boldsymbol{\theta} - \mathbf{f}(\mathbf{q}_{o})] \tag{21}$$

where (for the DOA problem),

$$f_i(\mathbf{q}_o) = \tan^{-1}\left(\frac{(y_o - y_i)}{(x_o - x_i)}\right). \tag{22}$$

3.1.2 Robust Method - Bearing Data

Suppose the errors are independently and identically distributed as the double exponential distribution (also known as the Laplace distribution), with known σ. That is,

$$\mathrm{p}(\boldsymbol{\theta}|\mathbf{q}) = \frac{\mathbf{1}}{2\sigma}\exp\left\{-|\boldsymbol{\theta} - \mathbf{f}(\mathbf{q})|\Big/\sigma\right\}. \tag{23}$$

Application of the maximum likelihood principle implies minimizing,

$$\zeta = \sum\left|\theta_{\mathrm{i}} - \mathrm{f}(\mathrm{q}_{\mathrm{i}})\right|. \tag{24}$$

Techniques which minimize the sum or mean of the absolute deviations in regression problems are referred to as MINMAD by Arthanari and Dodge [AD81]. Book has also pointed out that the least-absolute-deviations fix is the maximum likelihood estimate of the true position if the observation errors have the Laplace distribution [Boo82]. In

general robust processing refers to processing which attempts to mitigate the effects of noise distributions that are non-normal. This is the purpose of the MINMAD algorithms developed below and therefore they will be referred to as the robust algorithms to distinguish them from their least squares counterparts.

Substituting the truncated Taylor expansion,

$$\boldsymbol{\theta} - \mathbf{f}(\mathbf{q}) = \boldsymbol{\theta} - \mathbf{f}(\mathbf{q}_o) - \mathbf{G} \bullet (\mathbf{q} - \mathbf{q}_o) + \boldsymbol{\varepsilon}, \tag{25}$$

where $\boldsymbol{\varepsilon}$ includes the error from the approximation as well as from uncertainties in the measurements. Rearranging the R.H.S. of 25 results in a set of equations that can be used as constraints,

$$\begin{aligned} \mathbf{G}^{DOA}_{N_D x 2}\mathbf{q} + \boldsymbol{\varepsilon} &= \boldsymbol{\theta} - \mathbf{f}(\mathbf{q}_o) + \mathbf{G}^{DOA}_{N_D x 2}\mathbf{q}_o \\ \mathbf{G}^{DOA}_{N_D x 2}\mathbf{q} + \boldsymbol{\varepsilon} &= \mathbf{b}^{DOA}_{N_D x 1} \end{aligned}. \tag{26}$$

The following linear program minimizes the absolute value of the deviations in (26),

$$\min\left\{\mathbf{c}^T\begin{bmatrix}\mathbf{q}\\ \mathbf{e}\end{bmatrix}\right\} = \min\left\{\begin{bmatrix}0 & 0 & 1 & \cdots & 1\end{bmatrix}\begin{bmatrix} x \\ y \\ \pi_1 \\ \vdots \\ \pi_N \\ \nu_1 \\ \vdots \\ \nu_N \end{bmatrix}\right\} = \zeta^{DOA} \tag{27}$$

subject to,

$$\left[\begin{array}{c|c|c} \begin{bmatrix} \frac{-\sin(\phi_{o1})}{D_{o1}} & \frac{\cos(\phi_{o1})}{D_{o1}} \\ \vdots & \vdots \\ \frac{-\sin(\phi_{oN})}{D_{oN_D}} & \frac{\cos(\phi_{oN})}{D_{oN_D}} \end{bmatrix} & \begin{bmatrix} 1 & 0 & \cdots & \cdots & 0 \\ 0 & \ddots & & & \vdots \\ \vdots & & \ddots & & \vdots \\ \vdots & & & \ddots & 0 \\ 0 & \cdots & \cdots & 0 & 1 \end{bmatrix} & \begin{bmatrix} -1 & 0 & \cdots & \cdots & 0 \\ 0 & \ddots & & & \vdots \\ \vdots & & \ddots & & \vdots \\ \vdots & & & \ddots & 0 \\ 0 & \cdots & \cdots & 0 & -1 \end{bmatrix} \end{array}\right] \begin{bmatrix} x \\ y \\ \pi_1 \\ \vdots \\ \pi_{N_\Delta} \\ \nu_1 \\ \vdots \\ \nu_{N_\Delta} \end{bmatrix} = \mathbf{b}^{DOA}_{N_D x 1} \quad (28)$$

$$x, y, \pi_1, \cdots, \pi_N, \nu_1, \cdots, \nu_N \geq 0$$

Where $\mathbf{b}^{DOA}$ is given by the R.H.S. of (26). The π slack variables represent positive deviations and the ν surplus variables are negative deviations so that

$$\boldsymbol{\varepsilon} = \boldsymbol{\pi} - \boldsymbol{\nu} . \quad (29)$$

The error is composed of the difference of two positive quantities to satisfy the non-negativity conditions of the linear program. The restriction that *x* and *y* also be greater than zero can be accommodated by performing a coordinate translation using the nearby linear expansion point x_o,y_o to put the estimated position securely into the first quadrant.

The importance of various measurements can be chosen by changing the relative value of the objective function coefficients. Thus, the robust approach has the flexibility to accommodate measurements with different degrees of confidence by giving measurements with greater confidence a greater weighting.

The above formulation differs technically from the approach proposed by Book [Boo82] although the spirit of the two methods is the same in that both methods are attempting to minimize the sum of absolute deviations. Both methods search over all of the $N_D(N_D-1)/2$ intersection points to find a pair of bearing lines that minimizes the absolute error. The difference is that Book is using a cost function based on what has

come to be called the Stansfield algorithm [Sta47] which was originally derived from heuristic arguments and the assumption of small bearing measurement errors. If the initialization point $\mathbf{q}_o$ is close $\mathbf{q}$ then the linearized equations presented here are preferable to the Stansfield algorithm, which produces a larger estimator bias unless the bearing errors are small. However, if the bearing errors are large, it may not be possible to chose $\mathbf{q}_o$ close to $\mathbf{q}$. In this case, it is not clear which estimator is preferable. Young independently developed and presented essentially the same method of robust emitter location from DOA data as Book (in that it was based on the Stansfield equations) in [You96] prior to his knowledge of Book's work in this area.

3.2 Emitter Location From TDOA Data

Unlike the DOA problem there is less literature available for calculating a fix, robust or otherwise, from TDOA data (there is even less literature on FDOA which is to be discussed in the next section). This is understandable considering the history DOA has had in astronomy and geodesy. TDOA on the other hand requires better measurement, timekeeping and communication equipment than DOA and thus does not enjoy the literary hundred plus year lineage of the DOA problem which only requires the ability to measure an angle. However, this lack of a literary roots has not hindered TDOA applications in this century such as the LORAN and the Global Positioning System which have enjoyed enormous success. This section then will develop the linearized TDOA equations which will be used to form the robust TDOA location estimation algorithm based on linear programming.

3.2.1 Least Squares Method - TDOA Data

In TDOA systems the emitter is located by measuring the difference in arrival times between N stations having positions specified by the column vectors $s_1, s_2, \ldots s_N$. The emitter lies somewhere on a locus of points corresponding to constant difference in distance between any two stations. The two stations are the foci of a hyperbola. Figure 4 shows lines of constant TDOA between two receivers (represented by airplane icons although TDOA systems do not require receiver motion as does FDOA). The N stations yield N-1 difference measurements. The N-1 TDOA measurements are designated by N_T in the following development.

The TDOA measurements can be represented by

$$\boldsymbol{\tau} = \mathbf{H}\mathbf{d} / c + \boldsymbol{\varepsilon} \tag{30}$$

Where $\mathbf{d}$ is a N x 1 column vector of distances from the measurement stations to the transmitter and c is the propagation velocity of the wavefront. The column vector $\boldsymbol{\varepsilon}$ represents the errors in the TDOA measurements. The (N-1) x N matrix $\mathbf{H}$ has ones along the main diagonal and negative ones on the upper secondary diagonal,

$$\mathbf{H} = \begin{bmatrix} 1 & -1 & 0 & \cdots & 0 & 0 \\ 0 & 1 & -1 & \cdots & 0 & 0 \\ \vdots & \vdots & \vdots & & \vdots & \vdots \\ 0 & 0 & 0 & & 1 & -1 \end{bmatrix}. \tag{31}$$

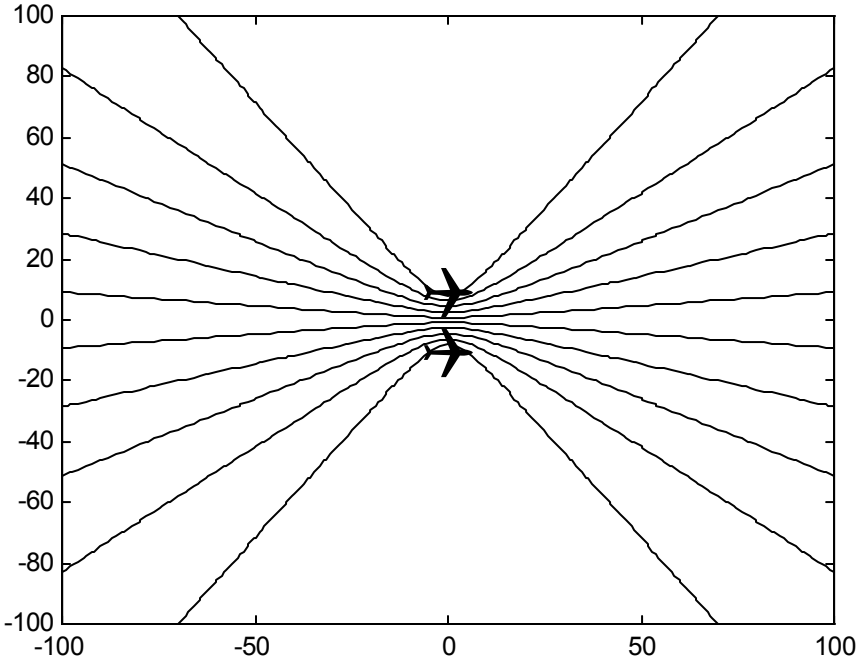

Figure 4 Lines of Constant TDOA.

Expanding (30**)** around a reference point $\mathbf{q_o}$,

$$\boldsymbol{\tau} = \mathbf{H}\,\mathbf{d_o}/c + \mathbf{G}^{\mathrm{TDOA}}_{N_T x 3}(\mathbf{q} - \mathbf{q_o}) + \boldsymbol{\varepsilon} \tag{32}$$

Where $\boldsymbol{\varepsilon}$ now also absorbs the error from the linear approximation and **G** for the TDOA problem is given by,

$$\mathbf{G}^{\mathrm{TDOA}}_{N_D x 3} = \left.\frac{d(\mathbf{H}\,\mathbf{d}/c)}{d(x,y,z)}\right|_{\mathbf{q_o}} = \mathbf{H}\left.\frac{d(\mathbf{d}/c)}{d(x,y,z)}\right|_{\mathbf{q_o}} = \mathbf{H}\mathbf{F}/c\,. \tag{33}$$

The first term of **F** is,

$$\mathbf{F}(1,1) = \left.\frac{\partial\left(\sqrt{(x_1 - x)^2 + (y_1 - y)^2 + (z_1 - z)^2}\right)}{\partial x}\right|_{x=x_o} = \frac{(x_o - x_1)}{\sqrt{(x_1 - x_o)^2 + (y_1 - y_o)^2 + (z_1 - z_o)^2}}$$

$$= \frac{(x_o - x_1)}{D_{01}}. \tag{34}$$

Where $D_{oi}=||\mathbf{q_o}-\mathbf{s_i}||$ denotes the distance from station i to the reference point. The y and z terms evaluate similarly so that **F** can be written as,

$$\mathbf{F} = \begin{bmatrix} (\mathbf{q_o} - \mathbf{s}_1) / D_{01} \\ \vdots \\ (\mathbf{q_o} - \mathbf{s}_{N_T}) / D_{0N_T} \end{bmatrix}. \tag{35}$$

Each row of **F** is a unit vector pointing from one of the stations to the reference point.

Applying (21) gives the linearized least squares solution for TDOA emitter location,

$$\hat{\mathbf{q}}^{TDOA} = \mathbf{q_o} + c(\mathbf{F}^T\mathbf{H}^T\mathbf{S}^{-1}\mathbf{H}\mathbf{F})^{-1}\mathbf{F}^T\mathbf{H}^T\mathbf{S}^{-1}[\boldsymbol{\tau} - \mathbf{H}\mathbf{d_o}/c]. \tag{36}$$

Where **S** is the error covariance of the TDOA measurements.

3.2.2 Robust Method - TDOA Data

Rearranging the linearized TDOA equation and using equation 33 for the derivative lets us write a system of equations that can be viewed as constraints in a linear program,

$$\begin{gathered} \frac{\mathbf{H}\mathbf{F}\mathbf{q}}{c} + \boldsymbol{\varepsilon} = \boldsymbol{\tau} - \frac{\mathbf{H}\mathbf{d_o} + \mathbf{H}\mathbf{F}\mathbf{q_o}}{c} \\ \mathbf{G}^{TDOA}_{N_T x 3}\mathbf{q} + \boldsymbol{\varepsilon} = \mathbf{b}^{TDOA}_{N_T x 1} \end{gathered} \tag{37}$$

The right side is a N-1 column vector derived from the station coordinates and the measured TDOA data. The error terms are treated as the difference of positive slack variables as before,

$$\boldsymbol{\varepsilon} = \boldsymbol{\pi} - \boldsymbol{\nu} \tag{38}$$

The following linear program minimizes the absolute value of the deviations,

$$\min\left\{\mathbf{c}^{\mathrm{T}}\begin{bmatrix}\mathbf{q}\\ \mathbf{e}\end{bmatrix}\right\} = \min\left\{\begin{bmatrix}0 & 0 & 0 & 1 & \cdots & 1\end{bmatrix}\begin{bmatrix}x\\ y\\ z\\ \pi_1\\ \vdots\\ \pi_{N_T}\\ \nu_1\\ \vdots\\ \nu_{N_T}\end{bmatrix}\right\} = \zeta^{\mathrm{TDOA}} \tag{39}$$

subject to,

$$\frac{1}{c}\left[\begin{array}{c|cccc|cccc} \dfrac{(\mathbf{q_o}-\mathbf{s}_1)}{D_{01}} - \dfrac{(\mathbf{q_o}-\mathbf{s}_2)}{D_{02}} & 1 & 0 & \cdots & 0 & -1 & 0 & \cdots & 0\\ \vdots & 0 & \ddots & & \vdots & 0 & \ddots & & \vdots\\ & \vdots & & \ddots & \vdots & \vdots & & \ddots & \vdots\\ \dfrac{(\mathbf{q_o}-\mathbf{s}_{N_T})}{D_{0N_T}} - \dfrac{(\mathbf{q_o}-\mathbf{s}_{N_T})}{D_{0N_T}} & 0 & \cdots & 0 & 1 & 0 & \cdots & 0 & -1 \end{array}\right]\begin{bmatrix}x\\ y\\ z\\ \pi_1\\ \vdots\\ \pi_{N_T}\\ \nu_1\\ \vdots\\ \nu_{N_T}\end{bmatrix} = \mathbf{b}^{\mathrm{DOA}}_{N_T x 1}$$

$$x, y, z, \pi_1, \cdots, \pi_N, \nu_1, \cdots, \nu_N \geq 0 \tag{40}$$

Where $\mathbf{b}^{\mathrm{TDOA}}$ is given by the R.H.S. of (37). The π slack variables represent positive deviations and the ν surplus variables are negative deviations. The restriction that *x* and *y* also be greater than zero can be accommodated by performing a coordinate translation using the nearby linear expansion point x_o,y_o to put the estimated position securely into the first quadrant.

The importance of various measurements can be adjusted by changing the relative value of the objective function coefficients.

3.3 Emitter Location From FDOA Data

Moving receivers can exploit the Doppler shift in several ways. The measured frequency at a receiver f_m is related to the transmitted frequency f_t by

$$f_m = f_t + f_t v_r = f_t + f_t v \cos(\varphi)/c \tag{41}$$

where c is the signal velocity, v_r is the velocity of the receiver in the direction to the transmitter, v is the receiver velocity, and φ is the bearing angle to the transmitter relative to the velocity vector, as shown in Figure 5. Therefore, the bearing angle can be

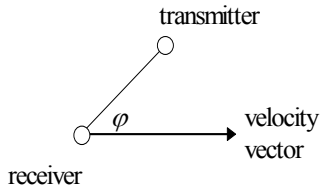

Figure 5 Moving receiver.

estimated if f_m is measured and f_t, v and c are known. Bearing measurements from several receivers can be combined to obtain a transmitter location estimate, as is done in Section A. Another approach, which may be less sensitive to inaccuracies in the assumed value of f_t, is to measure the Doppler difference, which is defined as

$$f_{m1} - f_{m2} = \left(f_t / c\right)\left(v_1 \cos(\varphi_1) - v_2 \cos(\varphi_2)\right) \tag{42}$$

where subscripts 1 and 2 refer to receivers 1 and 2 [Tor84]. The differential Doppler is defined as the integral of f_{m1}-f_{m2} over time. If f_t does not change too rapidly over the integration interval, the differential Doppler is

$$\int_{t_1}^{t_3} \left(f_{m1} - f_{m2}\right) dt \cong \left(f_{ta} \big/ c\right) \left[\left(D_1(t_2) - D_1(t_1)\right) - \left(D_2(t_2) - D_2(t_1)\right)\right] \tag{43}$$

where f_{ta} is the average transmitted frequency and $D_i(t_j)$, is the distance of receiver i from the transmitter at time j [Tor84]. The right-hand sides of 42 and 43 can be expressed in terms of the transmitter coordinates. Thus, in the absence of noise, a Doppler difference or a differential Doppler measurement determines a surface on which the transmitter must lie [Tor84]. Figure 6 shows lines of constant differential Doppler for two receivers traveling to the right at the same velocity.

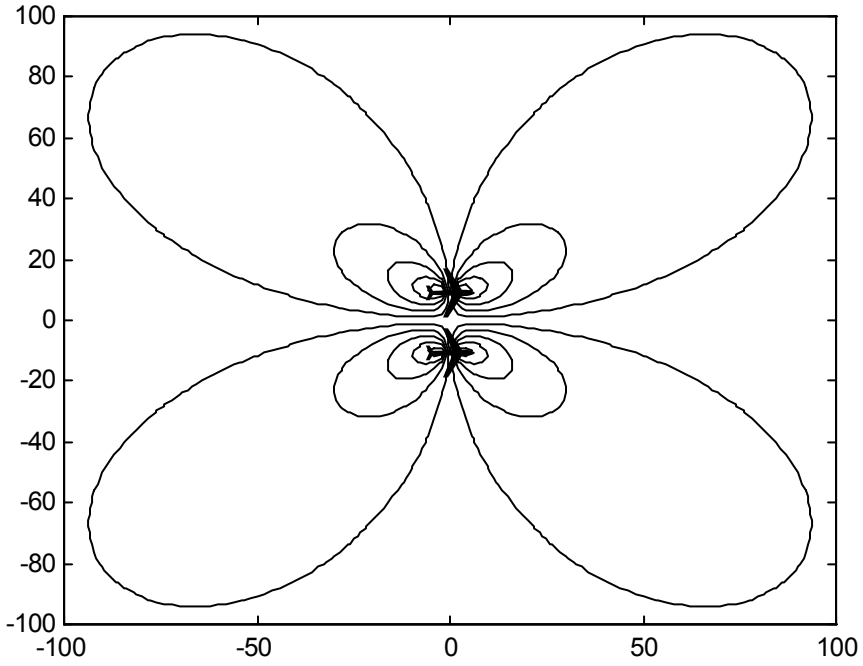

Figure 6. Lines of Constant Differential Doppler.

3.3.1 Least Squares Method - FDOA Data

In FDOA systems the emitter is located by measuring the Doppler difference or the differential Doppler in between N stations having positions specified by the column

vectors $s_1, s_2, \ldots s_N$. If differential Doppler is used the N-1 measurements can be represented by

$$\boldsymbol{\delta} = \left(f_{ta}/c\right)\mathbf{H}\left[\mathbf{d}(t_2) - \mathbf{d}(t_1)\right] + \boldsymbol{\varepsilon} \tag{44}$$

Where **d** is a N x 1 column vector of distances from the measurement stations to the transmitter at time t and c is the propagation velocity of the wavefront. The column vector $\boldsymbol{\varepsilon}$ represents the errors in the differential Doppler measurement vector $\boldsymbol{\delta}$. The N stations yield N-1 difference measurements over the integration period. The number of FDOA measurements is designated by N_F in the following development.

The N_F x N matrix **H** has ones along the main diagonal and negative ones on the upper secondary diagonal,

$$\mathbf{H} = \begin{bmatrix} 1 & -1 & 0 & \cdots & 0 & 0 \\ 0 & 1 & -1 & \cdots & 0 & 0 \\ \vdots & \vdots & \vdots & & \vdots & \vdots \\ 0 & 0 & 0 & & 1 & -1 \end{bmatrix}. \tag{45}$$

Expanding (30) around a nearby reference point $\mathbf{q_o}$,

$$\boldsymbol{\delta} = \left(\mathrm{f_{ta}}/\mathrm{c}\right)\mathbf{H}\left[\mathbf{d_o}(\mathrm{t}_2) - \mathbf{d_o}(\mathrm{t}_1)\right] + \mathbf{G}^{\mathrm{FDOA}}_{\mathrm{N_F x 3}}(\mathbf{q} - \mathbf{q_o}) + \boldsymbol{\varepsilon} \tag{46}$$

Where $\boldsymbol{\varepsilon}$ now also absorbs the error from the linear approximation and **G** is given by,

$$\begin{aligned} \mathbf{G}^{\mathrm{FDOA}}_{\mathrm{N_F x 3}} &= \left(\mathrm{f_{ta}}/\mathrm{c}\right)\frac{\mathrm{d}\left(\mathbf{H}\left[\mathbf{d}(\mathrm{t}_2) - \mathbf{d}(\mathrm{t}_1)\right]\right)}{\mathrm{d}(\mathrm{x},\mathrm{y},\mathrm{z})}\bigg|_{\mathbf{q_o}} = \left(\mathrm{f_{ta}}/\mathrm{c}\right)\mathbf{H}\frac{\mathrm{d}\left(\mathbf{d}(\mathrm{t}_2) - \mathbf{d}(\mathrm{t}_1)\right)}{\mathrm{d}(\mathrm{x},\mathrm{y},\mathrm{z})}\bigg|_{\mathbf{q_o}}. \\ &= \left(\mathrm{f_{ta}}/\mathrm{c}\right)\mathbf{H}\left[\mathbf{F}(\mathrm{t}_2) - \mathbf{F}(\mathrm{t}_1)\right] \end{aligned} \tag{47}$$

The first term of $\mathbf{F}(t_2)$ is,

$$\mathbf{F}_{11}(t_2) = \frac{\partial(\sqrt{(\mathrm{x}_1(t_2)-\mathrm{x})^2+(\mathrm{y}_1(t_2)-\mathrm{y})^2+(\mathrm{z}_1(t_2)-\mathrm{z})^2}}{\partial \mathrm{x}} \frac{1}{c}\Bigg|_{\mathrm{x}=\mathrm{x}_o}$$

$$= \frac{(\mathrm{x}_o - \mathrm{x}_1(t_2))}{\sqrt{(\mathrm{x}_1(t_2)-\mathrm{x}_o)^2+(\mathrm{y}_1(t_2)-\mathrm{y}_o)^2+(\mathrm{z}_1(t_2)-\mathrm{z}_o)^2}} \tag{48}$$

$$= \frac{(\mathrm{x}_o - \mathrm{x}_1(t_2))}{\mathrm{D}_{01}}$$

Where $D_{oi}=||\mathbf{q_o}-\mathbf{s}_i||$ denotes the distance from station i to the reference point. The y and z terms evaluate similarly so that **F**(t) can be written as,

$$\mathbf{F}(\mathrm{t}) = \begin{bmatrix} (\mathbf{q_o} - \mathbf{s}_1(\mathrm{t}))/\mathrm{D}_{01} \\ \vdots \\ (\mathbf{q_o} - \mathbf{s}_{\mathrm{N_F}}(\mathrm{t}))/\mathrm{D}_{0\mathrm{N_F}} \end{bmatrix}. \tag{49}$$

Each row of **F** is a unit vector pointing from one of the stations at time *t* to the reference point $\mathbf{q_0}$.

Applying (21) gives the linearized least squares solution for differential Doppler emitter location,

$$\hat{\mathbf{q}}^{\mathrm{FDOA}} = \mathbf{q_o} + \frac{\mathrm{c}}{\mathrm{f_{ta}}}\left(\left[\mathbf{F}(\mathrm{t}_2)-\mathbf{F}(\mathrm{t}_1)\right]^{\mathrm{T}}\mathbf{H}^{\mathrm{T}}\mathbf{S}^{-1}\mathbf{H}\left[\mathbf{F}(\mathrm{t}_2)-\mathbf{F}(\mathrm{t}_1)\right]\right)^{-1} \bullet \left[\mathbf{F}(\mathrm{t}_2)-\mathbf{F}(\mathrm{t}_1)\right]^{\mathrm{T}}\mathbf{H}^{\mathrm{T}}\mathbf{S}^{-1}\left[\delta - \mathrm{f_{ta}}\,\mathbf{H}\left[\mathbf{d_o}(\mathrm{t}_2)-\mathbf{d_o}(\mathrm{t}_1)\right]/\mathrm{c}\right] \tag{50}$$

Where **S** is the error covariance of the FDOA measurements.

3.3.2 Robust Method - FDOA Data

Rearranging the linearized differential Doppler equation and using equation 47 for the derivative lets us write a system of equations that can be viewed as constraints in a linear program,

$$\mathbf{H}\left[\mathbf{F}(t_2)-\mathbf{F}(t_1)\right]\mathbf{q}+\boldsymbol{\varepsilon}=\delta-\frac{f_{ta}}{c}\mathbf{H}\left[\mathbf{d}_o(t_2)-\mathbf{d}_o(t_1)\right]+\mathbf{H}\left[\mathbf{F}(t_2)-\mathbf{F}(t_1)\right]\mathbf{q}_o$$
$$\mathbf{G}^{FDOA}_{N_F x 3}\mathbf{q}+\boldsymbol{\varepsilon} \;=\; \mathbf{b}^{FDOA}_{N_F x 1} \qquad (51)$$

The right side is a N-1 column vector derived from the station coordinates and the measured FDOA data. The error terms are treated as the difference of positive slack variables as before,

$$\boldsymbol{\varepsilon}=\boldsymbol{\pi}-\boldsymbol{\nu}. \qquad (52)$$

The following linear program minimizes the absolute value of the deviations,

$$\min\left\{\mathbf{c}^T\begin{bmatrix}\mathbf{q}\\ \mathbf{e}\end{bmatrix}\right\}=\min\left\{\begin{bmatrix}0 & 0 & 0 & 1 & \cdots & 1\end{bmatrix}\begin{bmatrix}x\\ y\\ z\\ \pi_1\\ \vdots\\ \pi_{N_F}\\ \nu_1\\ \vdots\\ \nu_{N_F}\end{bmatrix}\right\}=\zeta^{FDOA} \qquad (53)$$

subject to,

$$\left[\begin{array}{c|ccccc|ccccc} & 1 & 0 & \cdots & \cdots & 0 & -1 & 0 & \cdots & \cdots & 0 \\ & 0 & \ddots & & & \vdots & 0 & \ddots & & & \vdots \\ \mathbf{H}\left[\mathbf{F}(t_2)-\mathbf{F}(t_1)\right] & \vdots & & \ddots & & \vdots & \vdots & & \ddots & & \vdots \\ & \vdots & & & \ddots & 0 & \vdots & & & \ddots & 0 \\ & 0 & \cdots & \cdots & 0 & 1 & 0 & \cdots & \cdots & 0 & -1 \end{array}\right]\begin{bmatrix} x \\ y \\ z \\ \pi_1 \\ \vdots \\ \pi_N \\ \nu_1 \\ \vdots \\ \nu_N \end{bmatrix} = \mathbf{b}^{\text{FDOA}}_{N_F x 1}$$

$$x, y, z, \pi_1, \cdots, \pi_N, \nu_1, \cdots, \nu_N \geq 0$$

(54)

Where $\mathbf{b}^{\text{FDOA}}$ is given by the R.H.S. of (51). The π slack variables represent positive deviations and the ν surplus variables are negative deviations. The restriction that *x* and *y* also be greater than zero can be accommodated by performing a coordinate translation using the nearby linear expansion point x_o,$y_{o,}$,z_o to put the estimated position securely into the region where the coordinates are positive.

The importance of various measurements can be adjusted by changing the relative value of the objective function coefficients.

Chapter 4

Updating the Emitter Location Solution

As new measurements are taken it is desired to update the current estimate of the emitter location. This can be done by adding a constraint for each new measurement. The new constraint will be satisfied by the current solution only in the unlikely event that the new measurement passes directly through the current solution. Otherwise the new constraint causes the current solution to be infeasible. Feasibility is recovered by augmenting the new constraint with the appropriate slack and surplus variables. Any basic variables in the constraint are substituted out using current non-basic variables. The current cost vector is appended with new coefficients corresponding to the new slack and surplus variables. Finally, the "modified" constraint is appended to the current optimum tableau and the dual simplex algorithm is used to recover feasibility [Tah92].

Example: Three bearing measurements are taken and the primal simplex solution computed for the estimated emitter location. Then a fourth bearing measurement is incorporated into the tableau and the dual simplex is used to update the solution.

The pertinent data is given in Table 1. Figure 7 shows the locations from which the bearing measurements are taken by the aircraft icons.

Table 1 X-Y and Bearing Data for Update Example

	self x-location (units of distance)	self y-location (units of distance)	bearing measurement (degrees)	bearing error (degrees)
observation 1	27.0	2.0	1.08	-0.1
observation 2	18.0	2.5	0.46	0.1
observation 3	10.0	3.0	0.00	-0.1
observation 4	8.0	3.5	-0.40	0.1

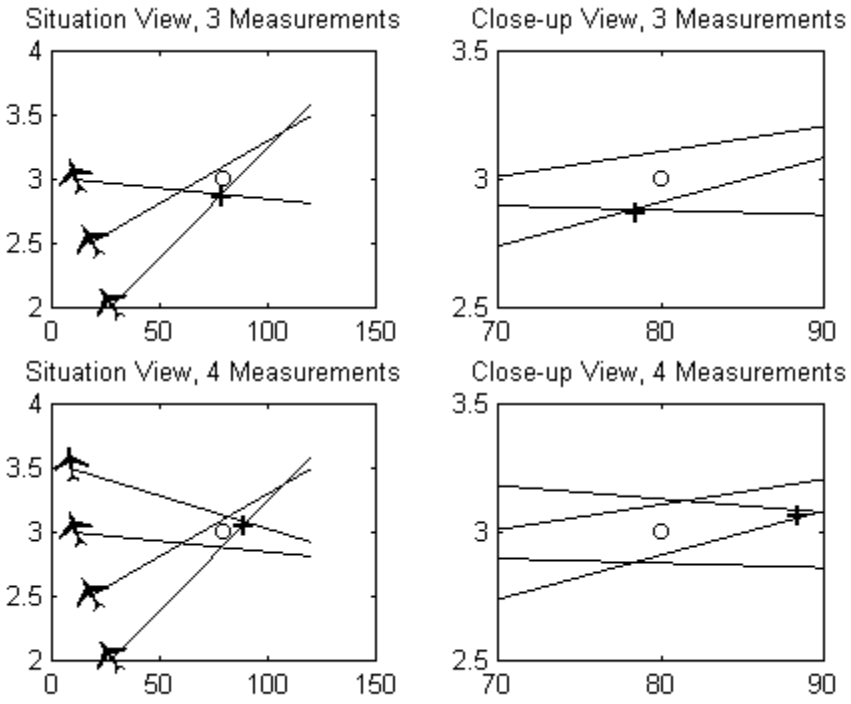

Figure 7 Illustration of Location Estimate Update.

Figure 3 depicts the orientation of the bearing measurements and the emitter. The emitter is represented by a circle. The location estimate is shown by the bolded plus symbol. The upper left drawing shows the first three bearing measurements in a "situation view" where emitter and measurement platform locations are visible. The

upper right drawing is a "close-up view" of the same data where only the region around the emitter can be seen. Likewise the bottom left drawing is the situation view after the fourth observation and the bottom right is the corresponding close-up view.

The construction of the initial tableau is straight forward. The elements of the **G** matrix are shown in the columns labeled x and y. The far right column corresponds to the **b** vector in equation 28. Each constraint row has a positive and negative slack variable in order to allow the overall deviation to be positive or negative.

Table 2 Initial Tableau with Three Observations

x	y	s_1	s_2	s_3	s_4	s_5	s_6	Solution
0	0	1	1	1	1	1	1	0
-0.0004	0.0189	1			-1			0.0264
-0.0001	0.0161		1			-1		0.0397
0.0000	0.0143			1			-1	0.0411

Table 4 shows the optimum tableau after solving using the primal simplex method.

Table 3 Solution after Primal Iterations

x	y	s_1	s_2	s_3	s_4	s_5	s_6	Solution
0	0	-1.366	0.0	-1.646	-0.634	-2.0	-0.3536	
0	1	0.0	0.0	70.0	0.0	0.0	-70.0	2.878
0	0	-0.4	1.0	-0.6	0.4	-0.1	0.6	0.0035
1	0	-2810	0.0	3710	2810	0.0	-3710	78.429

To update the solution after the fourth bearing measurement is taken it is necessary to replace any basic variables in the new constraint with current non-basic variables. The new constraint prior to substitution is

$$\mathbf{G}(4,1)\mathrm{x} + \mathbf{G}(4,2)\mathrm{y} + 0 + 0 + 0 + 0 + 0 + 0 + 0 + \pi_4 - \nu_4 = \mathrm{b}_4 \qquad (55)$$

recall that b_4 is derived from the bearing measurement and the linearization coordinates (x_o,y_o) via

$$\mathrm{b}_4 = \theta_4 - \tan^{-1}\left(\frac{(y_o - y_4)}{(x_o - x_4)}\right) + \mathbf{G}(4,1)\mathrm{x}_\mathrm{o} + \mathbf{G}(4,2)\mathrm{y}_\mathrm{o}\,. \qquad (56)$$

But the variables x and y in (55) are basic (from the previous optimal solution) and must be substituted out using the current non-basic variables. Rewriting the current solution for x and y in terms of non-basic variables,

$$\begin{aligned} \mathrm{x} &= \mathbf{b}^{\mathrm{opt}}(\mathrm{i}_\mathrm{x}) - \mathbf{A}^{\mathrm{opt}}(\mathrm{i}_\mathrm{x}, \mathbf{n}_{\mathrm{bas}}) \\ \mathrm{y} &= \mathbf{b}^{\mathrm{opt}}(\mathrm{i}_\mathrm{y}) - \mathbf{A}^{\mathrm{opt}}(\mathrm{i}_\mathrm{y}, \mathbf{n}_{\mathrm{bas}}) \end{aligned} \qquad (57)$$

where i_x represents the index of the row entry under the x column that contains a 1. Similarly i_y is the index of the entry in the y column that contains a 1. The vector $\mathbf{b}^{\mathrm{opt}}$ is the far right column vector from the previous optimum tableau. The matrix $\mathbf{A}^{\mathrm{opt}}$ is the main body of the previous optimum tableau. The vector $\mathbf{n}_{\mathrm{bas}}$ contains the indices of the non-basic variables in the previous optimum solution.

Substituting 57 into 55,

$$\mathbf{G}(4,1)[\mathbf{b}^{\mathrm{opt}}(\mathrm{i}_\mathrm{x}) - \mathbf{A}^{\mathrm{opt}}(\mathrm{i}_\mathrm{x}, \mathbf{n}_{\mathrm{bas}})] + \mathbf{G}(4,2)[\mathbf{b}^{\mathrm{opt}}(\mathrm{i}_\mathrm{y}) - \mathbf{A}^{\mathrm{opt}}(\mathrm{i}_\mathrm{y}, \mathbf{n}_{\mathrm{bas}})] + \pi_4 - \nu_4 = \mathrm{b}_4\,. \qquad (58)$$

Rearranging (58)

$$-\mathbf{G}(4,1)\mathbf{A}^{\mathrm{opt}}(\mathrm{i}_\mathrm{x}, \mathbf{n}_{\mathrm{bas}}) - \mathbf{G}(4,2)\mathbf{A}^{\mathrm{opt}}(\mathrm{i}_\mathrm{y}, \mathbf{n}_{\mathrm{bas}}) + \pi_4 - \nu_4 = \mathrm{b}_4 - \mathbf{G}(4,1)\mathbf{b}^{\mathrm{opt}}(\mathrm{i}_\mathrm{x}) - \mathbf{G}(4,2)\mathbf{b}^{\mathrm{opt}}(\mathrm{i}_\mathrm{y}) \qquad (59)$$

Equation (59) shows how to transform a new bearing measurement into a constraint that can be appended to the existing optimal tableau. Table 4 shows the modified constraint appended to the previous optimum tableau. The expanded tableau is now ready for dual simplex iterations.

Table 4 Modified Constraint Appended to Optimum Tableau

x	y	s_1	s_2	s_3	s_4	s_5	s_6	s_7	s_8	Solution
0	0	-1.366	0.0	-1.646	-0.634	-2.0	-0.3536	-1	-1	
0	1	0.0	0	70.0	0.0	0.0	-70	0	0	2.878
0	0	-0.4	1	-0.6	0.4	-0.1	0.6	0	0	0.0035
1	0	-2810	0	3710	2810	0.0	-3710	0	0	78.429
0	0	-0.3	0	1.3	0.3	0.0	-1.3	1	-1	-0.0036

Table 5 shows the optimum solution after the dual simplex.

Table 5 Solution Tableau after Update of New Constraint via Dual Simplex

	z	x	y	s_1	s_2	s_3	s_4	s_5	s_6	s_7	s_8	Solution
z		0	0	-1.293	0.	-2.0	-0.707	-2.000	0	-0.734	-1.266	0
		0	1	-14.3	0.0	0.0	-14.3	0	0	52.6	-52.6	3.0670
		0	0	-0.5	1	0	0.5	-1.0	0	-.5	0.5	0.0018
		1	0	-2054	0	0	2054	0	0	2790	-2790	88.4535
		0	0	0.2	0	-1.0	-0.2	0	1.0	0.8	-0.8	0.0027

The update example began with three constraints and added a fourth. However, the technique of writing the new constraint in terms of the existing non-basic variables and then using the dual simplex to recover feasibility can be easily applied whenever a new measurement arrives and it is desired to update an existing optimal solution.

Chapter 5

Measurement Association

The process of associating parameter data (e.g. DOA, TDOA, FDOA, modulation, frequency, etc.) to form a location estimate is one of data information fusion. Waveforms from various emitters are received and measured at multiple receiving stations. The receiving stations communicate their measurements to each other. The task of correctly assigning measurements to existing emitters (to obtain refined accuracy) or forming new emitter location estimates can be difficult when multiple (and perhaps simultaneous) emitters are present.

The advantage of minimizing the absolute value of the deviations versus the square becomes apparent when associating parameter data (DOA, TDOA, FDOA) into an emitter location estimate. The least-squares approach is overly sensitive to ambiguities or measurements from nearby emitter sites. On the other hand minimization of the absolute value of the deviations is robust to outliers and yields deviations that can be used to reject non-relevant measurements.

Example: LOB measurements are made from eight separate locations. The locations could represent either fixed ground sites or from one (or more) moving platforms. Six of the measurements are from an emitter with coordinates (3,100). The remaining are from a nearby emitter with coordinates (4,120). Table 2 gives the measurement platform(s) coordinates along with the bearing measurements. The bearing

noise was drawn from a normal distribution with zero mean and standard deviation of 0.1 degrees.

Table 6 X-Y and Bearing Data for Two Emitter Example

x-location (units of distance)	y-location (units of distance)	bearing (degrees)	bearing error (degrees)
0	0	1.7184	-0.0807
0	1	1.1458	-0.1130
0	2	0.5729	0.0204
0	3	0.0000	-0.0262
0	4	-0.5729	-0.0446
0	5	-0.4775	0.0593
0	6	-1.7184	0.0290
0	7	-1.4321	-0.0664

Figure 8 shows the bearing measurements and the estimated emitter location as computed by minimizing the absolute deviation. The robust method effectively discounts the two outliers and yields an accurate result for one of the emitters. On the other hand the least-squares emitter location is substantially affected by the outliers. The emitter one miss distance of the robust approach is 2.7 while the least-squares miss distance of 21.8 is over 8 times larger. Repeated independent trials with random bearing errors have confirmed the improved accuracy of robust relative to the least-squares approach.

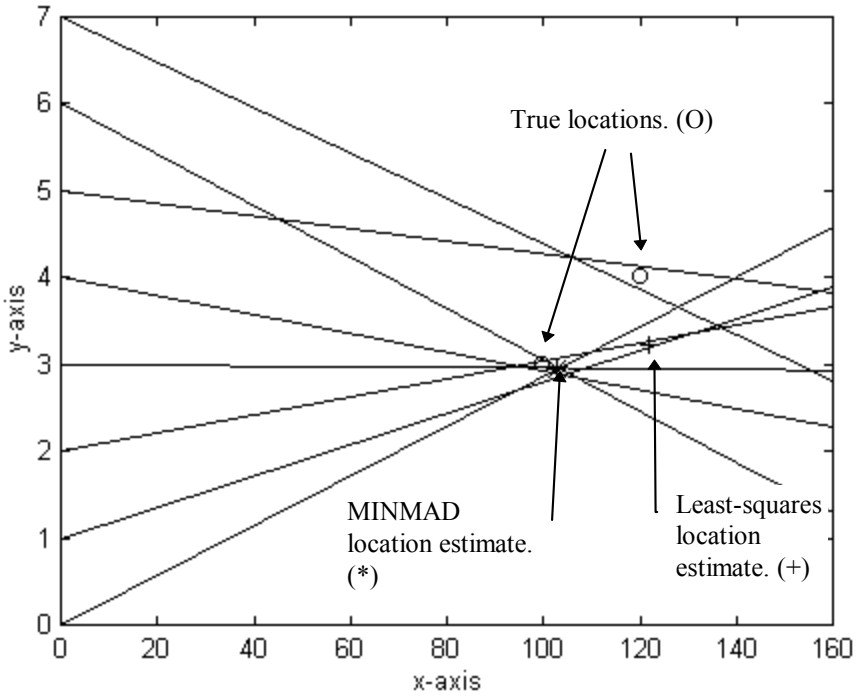

Figure 8 Situation View of robust and Least-Squares Comparison

Clustering algorithms calculate the distance between each point and every other point. Thus, for N points the processing load is on the order of $N^2/2$. Quick partition algorithms provide much greater efficiency.

Quick partition algorithms can be divided into two classes - Sorting and Leader. Sorting algorithms reorder the data by each parameter in turn and performs clustering on adjacent points. This requires as many passes through the data as there are variables [Mar88]. Leader algorithms require only a single pass through the data. The first point in the data is defined as a "leader". The distances between subsequent points and the leader are calculated. If the distance is less than the threshold the point is clustered, otherwise the point is defined as an additional leader. Subsequent points are compared with every leader until clustered or defined as a new leader.

The substantial accuracy improvement of the robust estimator simplifies separating the measurements into two groups because the robust location estimate provides a point that is easy to correlate the measurements to. Figure 9 compares the robust and least-squares deviations. If a threshold of 0.1 degrees is used to reject outliers then the measurements around the robust location estimate can be correctly associated using either one of the quick partition algorithms. However, using the same threshold around the least-squares location estimate results in observations 1,4,5 and 7 being misassociated regardless of the clustering algorithm used.

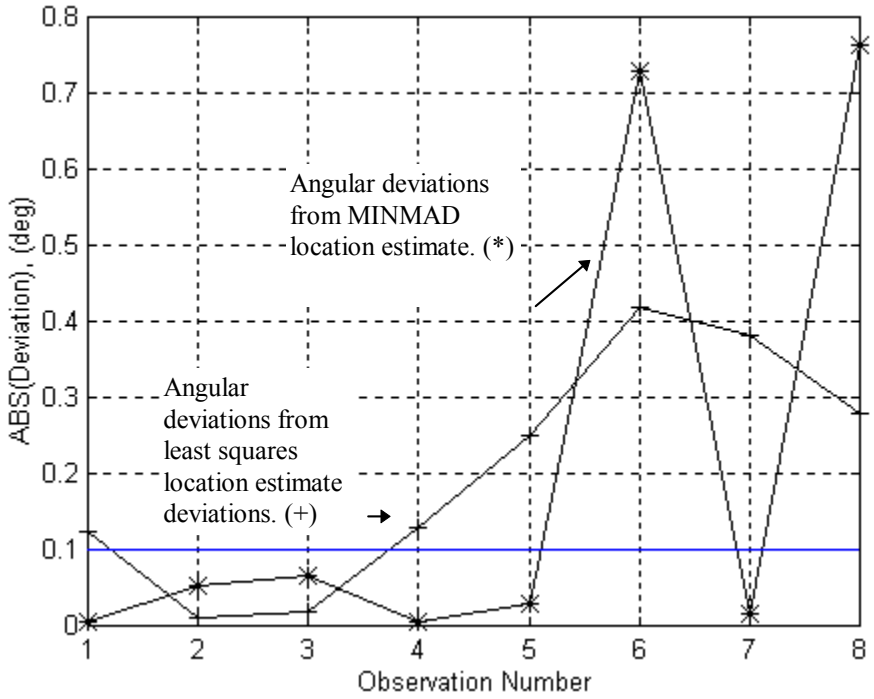

Figure 9 Comparison of robust and Least Squares Angular Deviations

Additional measurements such as modulation format and fine frequency are easily incorporated into the quick partitioning association process. While the additional information may assist in correct association, and thus effectively overcome the problems encountered with the least squares solution, the robust deviations will provide greater

cluster separation and larger noise immunity. Furthermore, it is possible that the additional measurements are either missing or do not provide any discrimination capability. That is it is possible that two emitters have the same modulation format and fine frequency so that the only remaining variable for discrimination is the deviation.

Chapter 6

Level 1 Information Fusion Architecture

A fusion model has been developed by the Department of Defense Joint Directors of Laboratories Data Fusion Subpanel to provide a framework and common reference for addressing data fusion issues and problems [WL90]. One of the models developed by the subpanel identifies three levels of fusion processing products:

Level 1 - Fused position and identity estimates.

Level 2 - Hostile or friendly military situation assessments.

Level 3 - Hostile force threat assessments.

Level 1 involves tracking, correlation, alignment, and association to yield position and identity estimates for targets or platforms in the composite filed of view. Level 1 processing operations are dominated by numeric procedures involving, for example, linear and nonlinear estimation techniques, pattern recognition processes, and various statistical operations.

Level 2 processing involves situation abstraction and assessment to yield a contextual interpretation of the distribution of forces produced in Level 1. Level 2 uses technical and doctrinal data bases to yield indications and warnings, plans of action, and inferences about the distribution of forces.

Level 3 processing is threat assessment. Threat assessment provides information concerning the *intent* of the hostile forces and the vulnerability of one's own forces. In addition it identifies threat opportunities through analysis of threat capabilities.

Level 1 processing is primarily numeric, involving linear and non-linear estimation techniques, pattern recognition processes, and various statistical operations. At Levels 2 and 3, the operations become dominated by symbolic reasoning processes involving various techniques from the field of artificial intelligence to support the formulation of higher levels of abstraction and inference. Clearly the robust approach to locating emitters falls into the Level 1 category because it is concerned solely with the numeric processing of the parameter data to yield identification and position estimation of radio emitters.

Obtaining a fused location estimate from separate DF, TDOA or FDOA measurements can be obtained by simply averaging the individual measurements together. However, better accuracy is possible if the measurements are processed jointly to yield a single fused location estimate result. The DF, TDOA and FDOA robust formulations described in Chapter 3 can be modified to accomplish a joint location estimator as follows. The individual models are stacked together to form a single large model:

Minimize,

$$\begin{bmatrix} 0 & 0 & 0 & \mathbf{1}_{1x2(N_D+N_T+N_F)} \end{bmatrix} \begin{bmatrix} x \\ y \\ z \\ \mathbf{e}_{2N_D x1} \\ \mathbf{e}_{2N_T x1} \\ \mathbf{e}_{2N_F x1} \end{bmatrix} = \zeta^{fusion}$$

with the following constraints,

$$\begin{bmatrix} \mathbf{G}^{DOA}_{N_D x3} & \mathbf{I}_{N_D} & -\mathbf{I}_{N_D} & \mathbf{0} & \mathbf{0} & \mathbf{0} & \mathbf{0} \\ \mathbf{G}^{TDOA}_{N_t x3} & \mathbf{0} & \mathbf{0} & \mathbf{I}_{N_T} & -\mathbf{I}_{N_T} & \mathbf{0} & \mathbf{0} \\ \mathbf{G}^{FDOA}_{N_F x3} & \mathbf{0} & \mathbf{0} & \mathbf{0} & \mathbf{0} & \mathbf{I}_{N_F} & -\mathbf{I}_{N_F} \\ \mathbf{0}_{1x3} & \zeta^{*TDOA}_{1xN_D} & \zeta^{*TDOA}_{1xN_D} & -\zeta^{*DOA}_{1xN_T} & -\zeta^{*DOA}_{1xN_Y} & \mathbf{0}_{1xN_F} & \mathbf{0}_{1xN_F} \\ \mathbf{0}_{1x3} & \zeta^{*FDOA}_{1xN_D} & \zeta^{*FDOA}_{1xN_D} & \mathbf{0}_{1xN_T} & \mathbf{0}_{1xN_T} & -\zeta^{*DOA}_{1xN_F} & -\zeta^{*DOA}_{1xN_F} \end{bmatrix} \begin{bmatrix} x \\ y \\ z \\ \mathbf{e}_{2N_D x1} \\ \mathbf{e}_{2N_T x1} \\ \mathbf{e}_{2N_F x1} \end{bmatrix} = \begin{bmatrix} \mathbf{b}^{DOA}_{N_D x1} \\ \mathbf{b}^{TDOA}_{N_t x1} \\ \mathbf{b}^{FDOA}_{N_F x1} \\ 0 \\ 0 \end{bmatrix}$$

$$x, y, z, e_i >= 0 \qquad \text{for i} = 1,\ldots,2(N_D + N_T + N_F)$$

Where the **G** and **b** terms have been defined in Chapter 3. The last two rows of the fusion model are constraints added to control the proportion that each measurement type (DOA, TDOA and FDOA) makes to the final solution [Bar97]. This is accomplished by first solving the individual robust models to obtain ζ^{*DOA}, ζ^{*TDOA} and ζ^{*FDOA}. For a given model solution ζ^* represents the minimum sum of absolute deviations. In the fused model it is unlikely that that each ζ will reach its ζ^*. Its proportion of the individual optima will be ζ / ζ^*. The fusion model requires that each sub-model's proportion of optimality be equal

$$\frac{\zeta^{DOA}}{\zeta^{*DOA}} = \frac{\zeta^{TDOA}}{\zeta^{*TDOA}} = \frac{\zeta^{FDOA}}{\zeta^{*FDOA}}.$$

Thus the last two rows in the fusion model correspond to

$$z^{*TDOA} z^{DOA} - z^{*DOA} z^{TDOA} = 0$$

and

$$z^{*FDOA} z^{TDOA} - z^{*TDOA} z^{FDOA} = 0. \tag{60}$$

If some of the submodels are more trusted than others, the constraints can be modified to reflect that. For example, if the DOA model was the most trustworthy, and the FDOA the least, then in place of 60 the following can be used

$$z^{*TDOA} z^{DOA} - z^{*DOA} z^{TDOA} \geq 0$$

and

$$z^{*FDOA} z^{TDOA} - z^{*TDOA} z^{FDOA} \geq 0. \tag{61}$$

Example: A Monte Carlo simulation study was undertaken to show the effectiveness of the robust fused model as well as the improvement of the individual robust submodels relative to least squares processing when the measurements contain outliers. The simulation involved four aircraft traveling at various speeds and headings. A stationary emitter of interest is located approximately 270 km distant to the east. The initial coordinates and velocities of the aircraft and emitter are given in Table 7.

Table 7 Coordinates and Velocities of Aircraft and Emitter.

	x -coordinate (m)	y -coordinate (m)	z-coordinate (m)	velocity (kmph)
aircraft 1	5,000	0	10,000	600@ 45.00°
aircraft 2	0	25,000	12,000	600@ 90.00°
aircraft 3	15,000	80,000	12,000	495@ 14.04°
aircraft 4	100,000	0	20,000	134@ 63.43°
emitter	300,000	50,000	0	0

An observation interval of 6 seconds was simulated. Each aircraft took measurements at the beginning, middle and end of the course it traversed during the observation interval. That is each aircraft took 3 DOA measurements. The TDOA and FDOA measurements are best described by examining the **H** matrices used for the simulation:

$\mathbf{H}_{TDOA}$ =

AC, position*	1,1	1,2	1,3	2,1	2,2	2,3	3,1	3,2	3,3	4,1	4,2	4,3
	1	0	0	-1	0	0	0	0	0	0	0	0
	1	0	0	0	0	0	-1	0	0	0	0	0
	0	1	0	0	-1	0	0	0	0	0	0	0
	0	1	0	0	0	0	0	-1	0	0	0	0
	0	0	1	0	0	-1	0	0	0	0	0	0
	0	0	1	0	0	0	0	0	-1	0	0	0
	0	0	0	1	0	0	-1	0	0	0	0	0
	0	0	0	0	1	0	0	-1	0	0	0	0
	0	0	0	0	0	1	0	0	-1	0	0	0
	1	0	0	0	0	0	0	0	0	-1	0	0
	0	0	0	0	0	1	0	0	0	0	0	-1
	0	0	0	0	0	0	0	1	0	0	-1	0

*The first number is the aircraft. The second number is its position during its course.

To interpret the $\mathbf{H}_{TDOA}$ matrix recall that each element of the vector $\mathbf{H}_{TDOA}\mathbf{d}$ is the differential distance between two points (aircraft in this case) and the emitter. For

example the first row of $\mathbf{H}_{TDOA}$ subtracts the distance of airplane two at time one from airplane one at time one.

The FDOA **H** matrix is interpreted similarly however each row of $\mathbf{H}_{FDOA}$ is a difference of differences. That is the first row of the $\mathbf{H}_{FDOA}$ matrix shown below represents the differential distance between aircraft two relative to the emitter at times one and two subtracted from the differential distance between aircraft one and the emitter at the same times. The $\mathbf{H}_{FDOA}$ matrix used in the simulation is shown below:

$\mathbf{H}_{FDOA}=$

AC, position*	1,1	1,2	1,3	2,1	2,2	2,3	3,1	3,2	3,3	4,1	4,2	4,3
	1	-1	0	-1	1	0	0	0	0	0	0	0
	1	-1	0	0	0	0	-1	1	0	0	0	0
	0	1	-1	0	-1	1	0	0	0	0	0	0
	0	1	-1	0	0	0	0	-1	1	0	0	0
	1	0	-1	-1	0	1	0	0	0	0	0	0
	1	0	-1	0	0	0	-1	0	1	0	0	0
	1	-1	0	0	0	0	0	0	0	-1	1	0
	0	0	0	0	1	-1	0	0	0	0	-1	1
	0	0	0	0	0	0	1	0	-1	-1	0	1

*The first number is the aircraft. The second number is its position during its course.

During the simulation the DOA measurements were processed first to yield an initialization point for subsequent processing. Since both the linearized least squares and the robust DOA formulation require an initialization point for the Taylor expansion an additional location method was developed that does not require an initialization point.

The DOA initialization routine selects one line of bearing from each of the three aircraft and calculates the vertices of the triangle formed by their intersections. The coordinates of the vertices are stored in a list in ascending order. This is repeated until every bearing measurement has been used. Each sorted list (there are three, one for each dimension) is then trimmed [BW84] by removing entries from both ends of the list in

order to limit the effect of outliers. Each trimmed list is then averaged and the resulting coordinates used as $\mathbf{q_o}$ in the subsequent DOA, TDOA and FDOA calculations.

In the simulation 100 trials were performed for two different cases. In the first case the error of all the DOA, TDOA and FDOA measurements were simulated to be normal zero mean with no outliers. The second set of trials however used a mixed mode distribution to generate the measurement noise so that a percentage of the measurements contained outliers. Equation 2 was used with the parameters in Table 8 to generate the measurement noise for each trial.

Table 8 Measurement Error Parameters for Mixed Mode Distributions.

	DOA	**TDOA**	**FDOA** (@1000 MHz)
μ_o	0^o	0 sec	0 Hz
μ_1	0.8^o	1.2 e^{-6} sec	40 Hz
μ_2	0.8^o	-1.2 e^{-6} sec	-40 Hz
σ_1	0.25^o	150 e^{-9} sec	5 Hz
σ_2	0.25^o	150 e^{-9} sec	5 Hz
σ_3	0.25^o	150 e^{-9} sec	5 Hz
α_1	0.0556	0.0556	0.0416
α_2	0.0556	0.0556	0.0416

Because understanding the simulation scenario from tables of coordinates and velocities is more difficult than simply glancing at a picture the following figures (10, 11 and 12) are given. The figures give a representative pictorial description of the magnitude of the errors used in the simulation and the shapes of the TDOA and FDOA curves

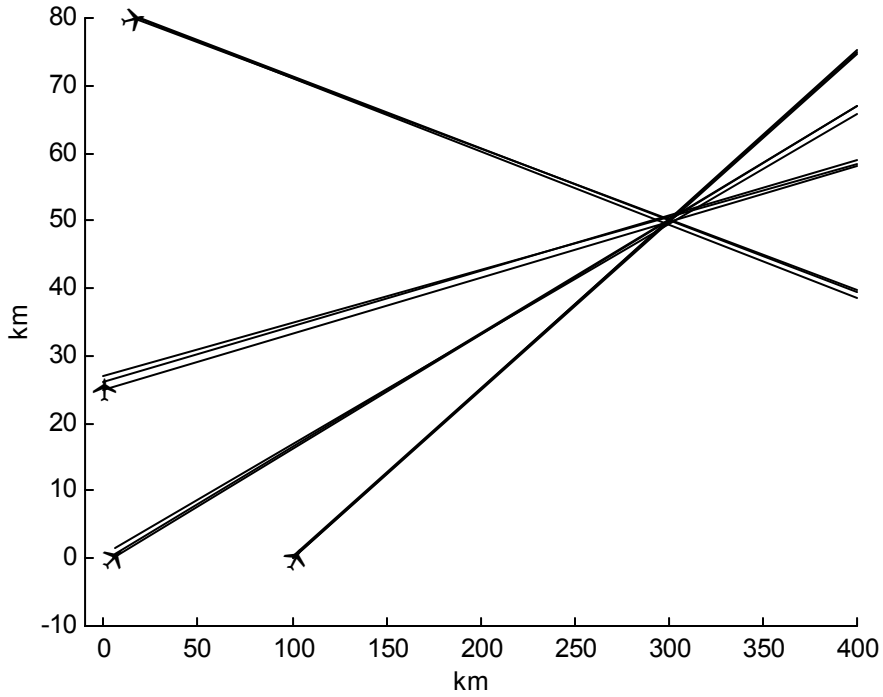

Figure 10 Simulation Scenario for DOA Measurements.

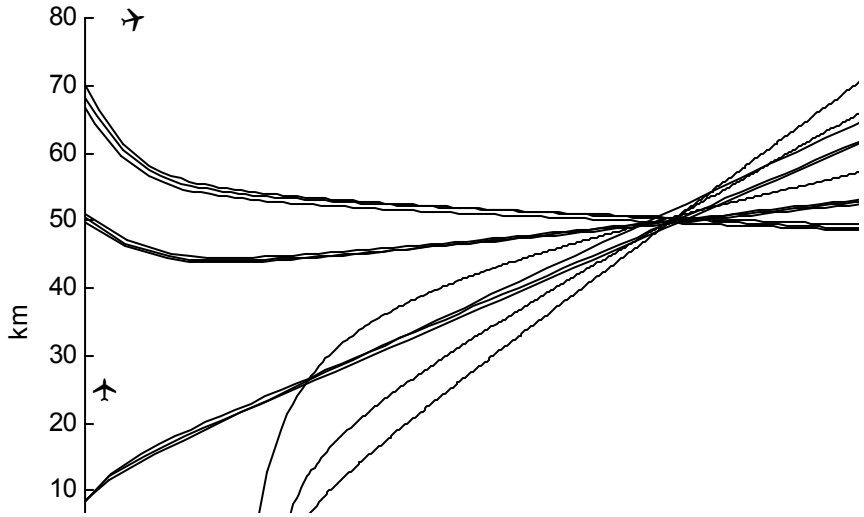

Figure 11 Simulation Scenario for TDOA Measurements.

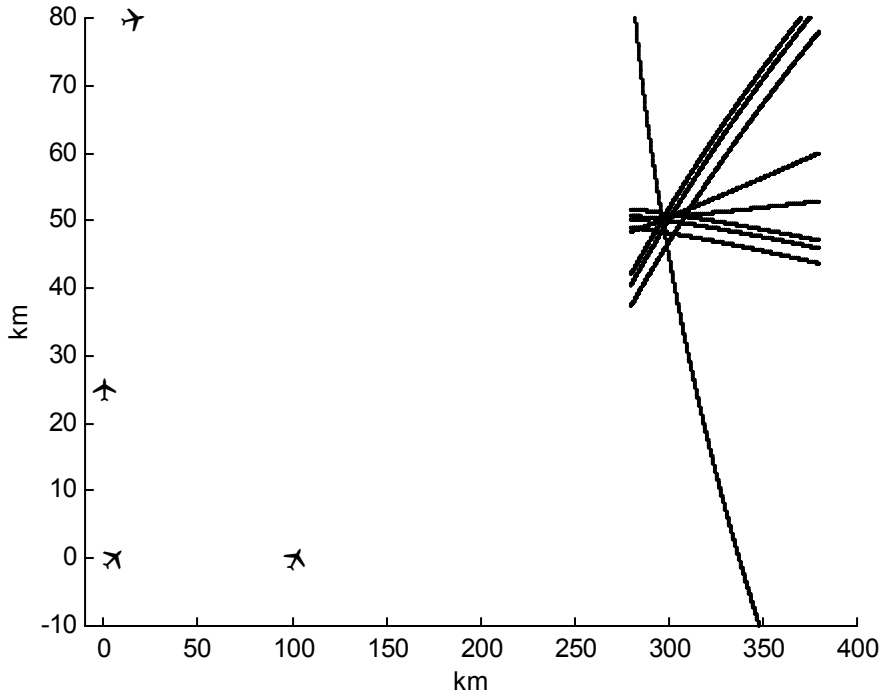

Figure 12 Simulation Scenario for FDOA Measurements.

To compare the various methods the distance from each location estimate to the true emitter location was saved for each of the 100 Monte Carlo trials. The saved errors were then used to compute a standard deviation of error for each method. The results of the simulation when only normally distributed noise was used (no outliers) is shown in Table 9. As is expected the robust method performs slightly worse than least squares in the absence of outliers. However, the robust fusion model result (800.3 meters) is significantly better than any of the individual least squares or robust results which shows the improved accuracy of the robust fusion model.

Table 9 Comparison of Least Squares to Robust Method when Measurement Noise is Normal

Normal Measurement Noise (no outliers)	Std. Dev. of Error (km) Least Squares	Std. Dev. of Error (km)

		Robust
DOA	1.2384	1.2392
TDOA	1.0402	1.1151
FDOA	0.8989	1.0440
Fusion		0.8003

However, the true value of the robust methods becomes apparent when outliers are present in the measurement data as was simulated in the second set of Monte Carlo trials. Table 10 shows this advantage. Each of the robust estimators out performs their least squares counterpart. Furthermore, the robust fusion method performs better than any individual estimator and is only slightly degraded (53 meters) relative to the case without outliers.

Table 10 Comparison of Least Squares to Robust Method when Measurement Noise Contains Outliers.

Mixed Mode Noise (see Table 8 and equation 2)	Std. Dev. of Error (km) Least Squares	Std. Dev. of Error (km) Robust
DOA	1.7728	1.5820
TDOA	2.2100	1.2707
FDOA	1.9778	1.3413
Fusion		0.8537

A Level 1 fusion architecture is proposed in figure 13 which utilizes robust, least squares and quick partitioning algorithms. The parameter measurements are made from various sensors distributed throughout the environment. The measurements are sent to a central processing point where the first step is association with existing emitter sites. If a measurement successfully associates with an existing site then it is stored in the Correlated Parameter Storage area, otherwise it is placed in Uncorrelated Parameter

Storage. Measurements in Correlated Parameter Storage are submitted to the Least Squares Refinement processing in order to update the location of the existing emitter sites. Uncorrelated measurements are processed by the robust fusion method. The deviations from robust fusion processing along with modulation format and fine frequency are passed to the Quick Partitioning algorithm. The resulting partitions are candidate emitter sites. Qualification of a partition depends on the number of measurements in it and the degree of dispersion between the measurements. If a partition satisfies these requirements it is upgraded to new site status and the measurements are placed in Correlated Parameter Storage (where they will be accessed by Least Squares Refinement).

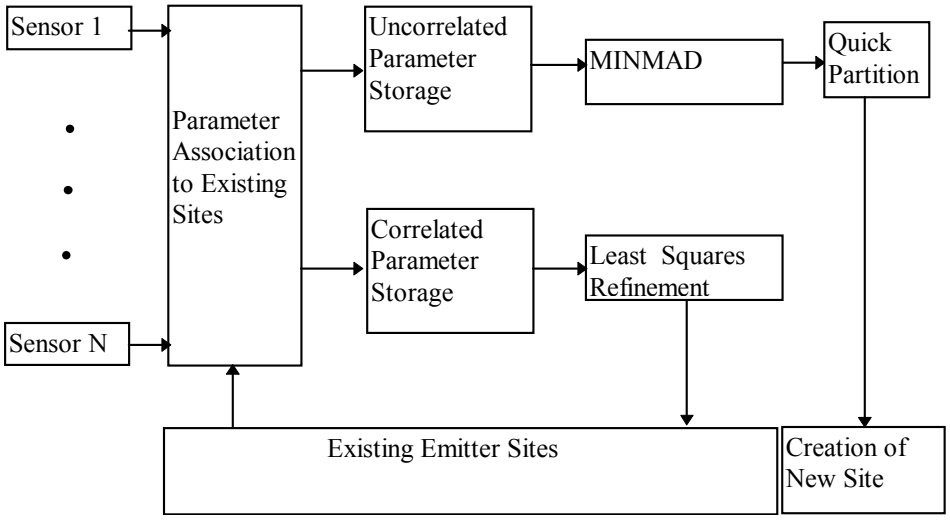

Figure 13 Level 1 Information Fusion Architecture Utilizing robust

Once a group of measurements have been removed from Uncorrelated Parameter Storage and associated with a new site the robust processing can be repeated to on the remaining measurements. This process is repeated until no new sites can be created. As new measurements that fail to correlate to existing sites arrive, the update equations

described in Chapter 4 are used to update the optimum robust fusion solution. The new solution is then used by the partition algorithms to check for new site creation.

Chapter 7

Economic Analysis

Comparison of algorithms solely on the basis of their performance in areas of computational load, memory usage, input/output requirements and statistical and numerical properties without considering their impact on the overall system in a cost-benefit sense may lead to false conclusions. The usual assumption is that the algorithm that exhibits the best statistical and numerical properties while expending the least computational resources is the one to be preferred. However computational resources can be directly converted to a monetary value by using the current price of processing and memory devices and conversion of statistical performance into an economic quantity can be accomplished given enough knowledge of the application. After conversion, the true costs and benefits of the algorithm application can be considered for proper algorithm selection. In many cases performance is paramount and implementation costs become an issue only when they exceed available funding levels. This has been the history of many military applications of the past where performance was everything. Recent procurement reform however has stressed cost as an independent variable (CAIV). CAIV is defined as the following in [USN97]:

> "CAIV is a key acquisition reform initiative. It entails setting aggressive, realistic cost objectives for systems and managing risks to obtain those objectives. The cost objectives should balance mission needs with available and projected resources, taking into account the state of requisite technologies. Bottom line: once system performance and objective costs are decided, through cost-performance trade-offs, cost becomes more of a constraint and less of a variable in meeting the mission need."

The emphasis is on cost-benefit analysis to determine aggressive cost targets early in the development cycle followed by careful management of risks to meet the cost objectives.

In this chapter a method will be determined for developing cost objectives for the implementation of the fusion architecture presented in Chapter 6. To develop the economic analysis for the fusion architecture we will first play the role of the government and use the concept of CAIV to establish a performance versus cost curve. Any point on this curve represents a cost and performance pairing that is acceptable to the government. Then we will switch to the role of the contractor and show how to perform algorithm selection and system sizing in such a way as to maximize profit while simultaneously minimizing risk and meeting the governments cost and performance objectives.

7.1 Performance as a Function of Cost

Defining an acceptable performance as a function of cost is not easy because overall performance is difficult to reduce to a single number. Moreover stating acceptable performance levels as a function of cost requires making difficult decisions. These decisions can sometimes literally involve probabilities of life and death . This unpleasant difficulty is probably why the issue has previously been ignored and the grail of total performance has been pursued at the expense of cost overruns.

However for the fusion architecture of the previous chapter a performance-versus cost-curve can be constructed in a straightforward manner. The rationale hinges on the extra cost of wastefully expending missile munitions on targets that are poorly located. Assume that the targeting algorithm error is a circular normal random variable with an

RMS value denoted by σ_a. Let the missile also have a normally distributed circular error denoted by σ_m. The error distribution of the weapon system is the root sum of squares (RSS) of the targeting system error and the missile error:

$$\sigma_t = \sqrt{\sigma_a^2 + \sigma_m^2} \,. \tag{62}$$

Let the government requirement be that on average at least one or more missiles must strike within a radius R of the target with a probability p_r. The probability that a single missile will strike within the radius R is

$$p_1 = \frac{2}{\sqrt{\pi}} \int_0^{R/\sigma_t} \exp^{(-x^2)} dx = \text{erf}\left(R/\sigma_t\right) . \tag{63}$$

If M missiles are launched, the probability that none of them fall inside the radius R is $(1\text{-}p_1)^M$. The probability that one or more will fall inside the radius is

$$p_r = 1 - \left(1 - p_1\right)^M \tag{64}$$

Solving for M gives the average number of missiles needed to meet the probability requirement of at least one missile inside the radius R

$$M = \frac{log\left(1 - p_r\right)}{log\left(1 - p_1\right)}. \tag{65}$$

Thus as the targeting error σ_a decreases the probability of a single missile meeting the requirement increases so that fewer total missiles are required.

To establish the performance-cost curve for the targeting system we will assume each missile has a cost of C_m and that the expected number of targets engaged per year is N_t over a useful system life of Y years. Using interest rate i and (62), (63) and (65) we can calculate the net present value of the missile costs as a function of the error

$$\mathrm{NPV}(\sigma_t) = \frac{\mathrm{C_m}\log(1-p_r)\mathrm{N}_t\left(\left(1-(1+i)^{-\mathrm{Y}}\right)/i\right)}{\log\left(1-erf\left(\frac{R}{\sigma_t}\right)\right)} \tag{66}$$

To quantify the value of a new higher accuracy targeting system assume the government has access to an existing targeting system capable of meeting the requirement with $\mathrm{M_{old}}$ missiles. The Net Present Value of the savings derived from a new targeting system with lower error σ_t is the cost of the extra missiles over the life of the system. The potential savings represents the equivalent cost C the government could incur for a new targeting system is:

$$C = \mathrm{C_m N_t}\left(\left(1-(1+i)^{-\mathrm{Y}}\right)/i\right)\left(\mathrm{M_{old}} - \frac{\log(1-p_r)}{\log\left(1-erf\left(\frac{R}{\sigma_t}\right)\right)}\right). \tag{67}$$

Rearranging the above equation so that cost is an independent variable gives the targeting error as a function of cost,

$$\sigma_t = R\left[inverf\left(1-\exp\left[\frac{\log\left((1-p_r)\right)}{\mathrm{M_{old}} - \frac{C}{\mathrm{C_m}\left(\left(1-(1+i)^{-\mathrm{Y}}\right)/i\right)\mathrm{N}_t}}\right]\right)\right]^{-1} \tag{68}$$

A recurrent problem in communicating about algorithms is the fact that we want to talk about algorithm accuracy performance and yet we measure its error which is inversely related to performance. That is, the higher performing algorithm has the lower error. To avoid the semantic confusion define performance as follows

$$P = -10\ log_{10}(\sigma)\,. \tag{69}$$

Using (70) and the above definition we can express the government's required system performance P_g as a function of equivalent cost C:

$$P_g = 10\log_{10}\left(R\left[inverf\left(1-\exp\left[\frac{\log(1-p_r)}{\mathrm{M_{old}} - \frac{C}{\mathrm{C_m}\left(\left(1-(1+i)^{-\mathrm{Y}}\right)/i\right)\mathrm{N}_t}} \right] \right) \right]^{-1} \right). \qquad (71)$$

7.2 Maximizing Profit with Performance and Cost Constraints

The model developed in this section uses a contractor's performance-versus-cost curve, where the performance and cost is derived from size and speed of the targeting system over its useful life. The contractor's curve is then compared to the government's curve. The project is feasible for all performance values on the contractor's curve that exceed the government's curve however the maximum profit point is found by taking into account risk considerations.

In the following model, system cost and algorithm performance are related through the error reduction obtained by increasing the number of independent observations. Specifically if the system hardware and software are modified to allow an increase by a factor of N independent measurements then the resulting standard deviation of error of the averaged results will be decreased by $\sqrt{\mathrm{N}}$. For example if the hardware is doubled (and if the system is perfectly scaleable) then number of independent measurements can double and the standard deviation of error σ_a can be decreased by $\sqrt{2}$.

Let the minimum system costs and associated error σ_o be related to the actual cost and error via

$$C = k_s C_{HW}^{RE}\left(\frac{\sigma_a^2}{\sigma_o^2} - 1\right) + C_{HW}^{RE} + C_{HW}^{NRE} + C_{SW}\,. \tag{72}$$

Where k_s represents the scaleability of the system. A k_s value greater than one can be used to model the penalty associated with the extra overhead of a larger system. Values of k_s greater than one allow for the fact that doubling the system size may not result in a doubling of the computation rate because of the extra work of communicating the problem to and assembling the results from the additional processors. C_{HW}^{RE} and C_{HW}^{NRE} represent the recurring and non-recurring portions of the hardware development, respectively. A scaleable design avoids non-recurring charges when scaling to a larger system. The software development is treated as completely non-recurring although k_s can be increased to account for the extra expense of algorithmic software that does not scale up easily.

Solving (72) for the system standard deviation of error and applying the definition of performance

$$P_c = -10\,log_{10}\left(\sqrt{\sigma_o^2\,\frac{C - C_{HW}^{RE} - C_{HW}^{RE} - C_{SW}}{k_s C_{HW}^{RE}} + \sigma_m^2}\right). \tag{73}$$

The intersection(s) of the government's performance-cost curve with the contractor's can be found by equating the above equation with equation (71) and solving for *C*. Finding the solution for the intersection of the P_c and the P_g curves requires trial and error techniques. However plotting the two curves over the interval of interest gives an easy indication of the number of roots and also provides a starting point for an iterative solution technique.

If the contract is structured so that profit is a percentage of the cost then it is in the contractor's interest to propose a maximum cost system. However the maximum cost system may not possess the maximum performance margin over the customer's requirements. Any slip in the ability of the contractor to meet the performance requirements may result in an unacceptable system. The cost of an unacceptable system may take the several forms. Unfunded contract overages to fix the problem may be required as well as customer imposed penalties. Loss of customer goodwill and the potential liability of delivering an inadequate system may also be incurred. Let these costs be lumped together under the term performance risk costs, C_r. It is reasonable to suppose that risk costs decrease for a system which has increasing performance P_c over and above the government's requirements P_g so that the expected profit is the contractor's fee minus the risk cost. The contractor's fee is a percentage p of the system cost. However the contractor's profit S is the percentage fee, pC, minus the performance risk costs:

$$S = pC - C_r . \tag{74}$$

Devising a suitable model for risk cost is a complex problem, however, for the purpose of selecting algorithms and sizing the system the following risk cost model is proposed:

$$C_r = pC\left(1 - \left(\frac{P_c - P_g}{k_r}\right)\right) = pC(1 - R) \tag{75}$$

The constant k_r is adjusted to reflect the importance of performance margin. For example if k_r is set to be equal to the maximum performance margin then the risk cost is

zero at the system cost point at which the maximum margin occurs. Substituting (75) into (76) gives the expected profit as a function of system cost and risk:

$$S = pCR \tag{77}$$

Analytically solving for the system cost that yields maximum profit requires taking the derivative of equation 78 which is daunting because of the inverse error function in the performance equations. However, profit as a function of system cost can be easily plotted to yield a graphical estimate of the optimum system cost as is illustrated in the following example.

7.3 Fusion Architecture Example

To illustrate the above concepts consider the fusion architecture of the previous chapter. We will develop the government's required performance as a function of cost curve by assuming values for R, p_r, M_{old}, C_m, i, N_t, Y and σ_m. Then we will compare two different contractor curves, one based on a fusion architecture with the robust emitter location capability and the other a fusion architecture without the robust algorithms.

To develop the government's curve assume that the current system is capable on average of delivering at least one missile out of four within a 300 meter radius with a probability of 0.95. Assume the current weapon accuracy is 100 meters. Thus, R=200 meters, p_r=0.95, M_{old}=4 and σ_m=100 meters. Assume each missile costs $80,000 and that 100 targets per year are to be engaged over a 10-year system life. Using a discount rate of 6%, (71) can be used to calculate the government's required performance as a function of cost as shown in Figure 14. The curve terminates at around $88,000,000 because increased performance beyond this point results in less than one missile per target (i.e.,

there is a point in targeting accuracy performance beyond which it is not economically worthwhile to pursue because the increased accuracy becomes irrelevant).

To compare the contractor's performance curves, we must estimate the minimum implementation cost and performance for both architectures. The minimum implementation is defined as the smallest realization of the system that can be linearly scaled upward. It includes the cost of hardware and software development. Table 11 gives estimates of the relevant parameters for both architectures.

Table 11 Cost Estimation Parameters for Two Architectures (dollars in thousands)

Parameter	Parameter value without robust processing.	Parameter value with robust processing.	Comment
σ_o	2000 meters	850 meters	Robust processing decreases the base error.
P_o	-33.01	-29.29	Robust processing increases the base performance.
C_{HW}^{RE}	$100	$400	Minimum robust implementation requires substantially more computing capacity.
C_{HW}^{NRE}	$200	$300	Hardware NRE is slightly more for robust implementation.
C_{SW}	$2000	$5000	Robust software is more than twice as complex.
k_s	1.1	1.1	Scaling parameter -no difference.
k_r	1.7	1.7	Risk parameter -no difference.
p	0.10	0.10	Profit percentage is 10%

Equation 73 and the parameters in the above table have been used to produce the two system performance curves depicted in figure 14. The robust processing performance curve has better performance at all cost values above $12,500,000 than the system without robust processing.

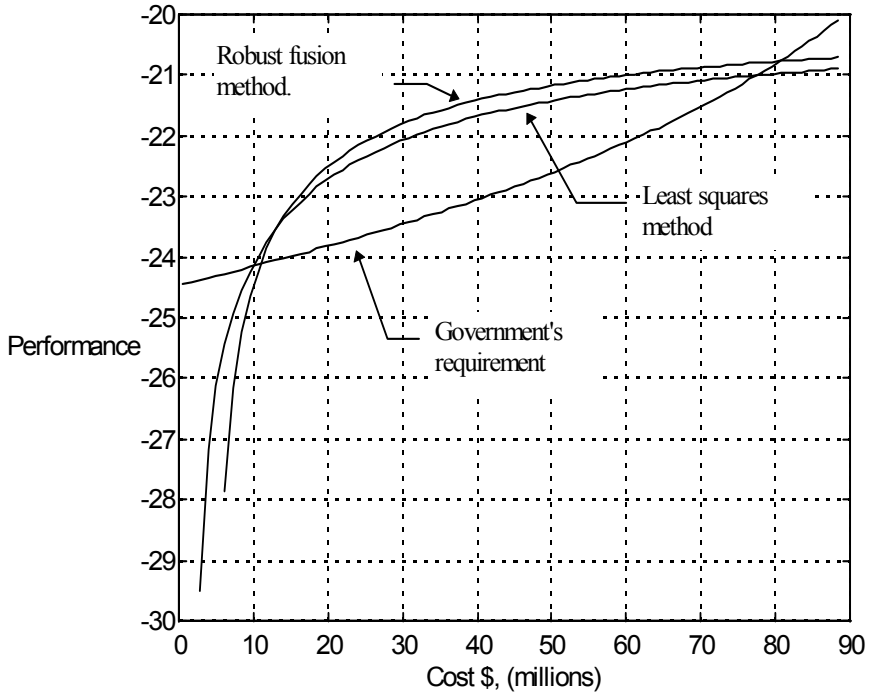

Figure 14 Performance as a Function of Cost.

The difference between the contractor's system performance and the government's required performance is related to the risk cost as described in 75. The risk cost is plotted in figure 15 for both systems. The risk cost is small in the mid region because the performance of the both systems exceeds the requirement to such an extent that the likelihood of not meeting the requirement is small. However, as each system's performance curve nears the government's requirement curve the risk cost increases as can be seen in the figure.

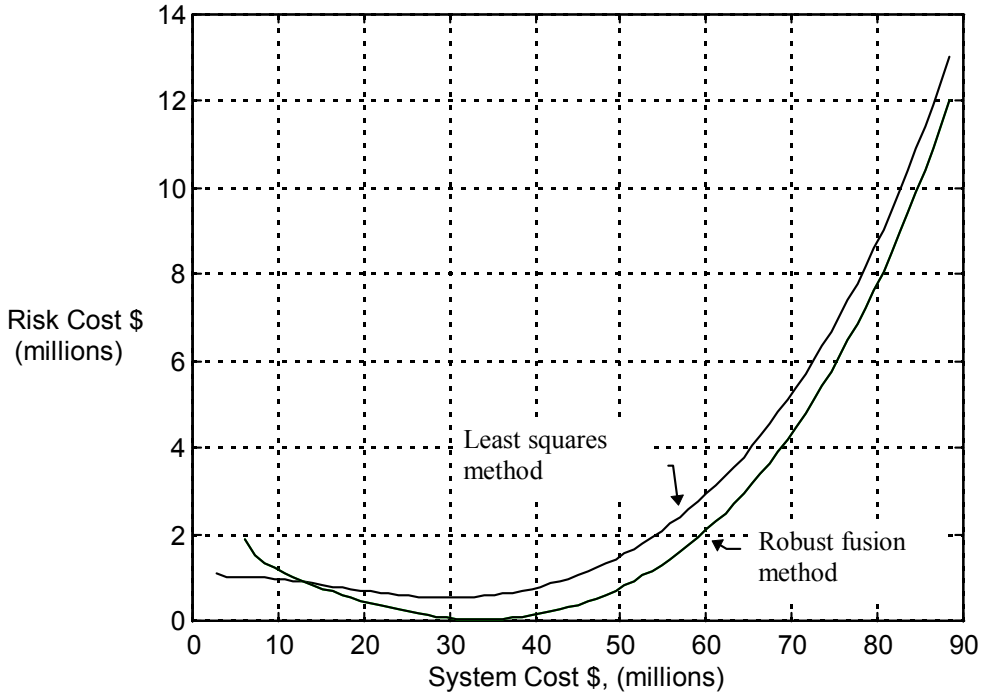

Figure 15 Risk Cost as a Function of System Cost.

Equation 15 along with the parameters in Table 11 give the two profit curves shown in figure 17. Note that the minimum risk points as shown in Figure 14 do not correspond with the maximum profit points of Figure 15 (i.e. some risk must be incurred to achieve maximum profit). The maximum profit of the system with robust processing is $4,229,900 which is $737,928 greater than the system without robust processing.

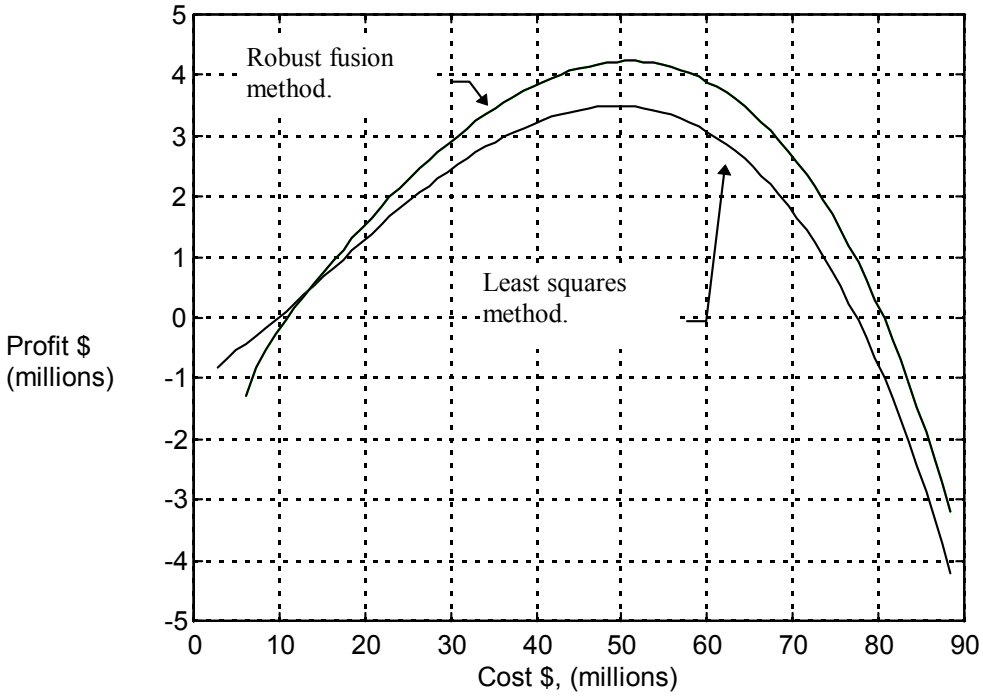

Figure 16 Profit as a Function of System Cost (Risk Adjusted).

The example shows the value of the proposed economic models for evaluating the contribution of algorithmic performance to overall system value and profit. The model has been demonstrated to have the ability to factor in the risk and scaleability of the system under consideration using cost as an independent variable. By applying the model to a set of sample parameters it has been possible to show how to perform algorithm selection and system sizing to maximize profit while simultaneously minimizing risk and meeting the government's cost and performance objectives.

Chapter 8

Conclusions

The ability of improved sensor systems to generate a veritable flood of location parameter data (e.g. DOA, TDOA, FDOA, etc.) demands new and automatic techniques for automatically associating the measurements with emitters. Problems arise using least squares emitter location when the measurements do not all belong to the same emitter or when ambiguities cause outliers. The minimization of the absolute error on the other hand can withstand contamination of this sort and still yield accurate location estimates.

A robust linear programming formulation which minimizes the mean of absolute deviations has been given for DOA, TDOA and FDOA data. Update equations have been derived which allow computation of the robust location estimates in real time as measurements are taken.

The linear program approach is robust to outliers and is therefore highly appropriate in a Level 1 fusion environment for obtaining initial location estimates. A Level 1 fusion architecture has been described which uses a fused robust location estimation formulation of all available information (DOA, TDOA and FDOA) together with quick partitioning algorithms to reject outliers arising from ambiguities or other emitters. The robust fusion method was shown to be significantly more accurate than processing the same data with any of the least squares methods.

The absolute deviations and other measurements such as modulation format and fine frequency are also used in the quick partitioning algorithm to associate a subset of measurements with a new candidate emitter location. Once a subset of measurements has passed the partitioning algorithm then least-squares estimation is used to obtain a refined location.

8.1 Future Work

The accuracy of any emitter location system is dependent on the geometry of the receiving stations relative to the emitter. Estimating the accuracy contours for a given geometry of receiving stations requires sophisticated analysis. This is important especially for military applications because certain geometries are pathologic containing "black holes" which prevent the location system from obtaining a fix. Fortunately accuracy analysis has been performed for the linearized least squares estimators by Torrieri [Tor84] for normally distributed errors. However, analytically deriving the performance of either the least squares or the robust approach in the presence of a mixed noise distribution is more difficult although Book [Boo82] has proposed (for the DOA problem only) an interesting method for computing the confidence that the true location lies within the largest polygon formed by the k direction lines nearest to the estimated median point. A first step in obtaining useful performance predictions may be to verify Book's confidence level formulas via Monte Carlo simulation using various mixed noise parameters.

A majority of location systems (and literature) are based upon some sort of Kalman filtering structure (e.g. extended or iterated extended). The Kalman filtering

approach has proven itself in many application domains because of its ability to track changing parameter values which in the present application corresponds to moving targets, which is of course of immense interest. However the Kalman filter structure is not inherently better than least squares unless the parameters are changing during the observation interval. If the parameters are changing slowly then batch processing (least squares or robust) can track the changes block by block.

Kalman filters may have some degree of robustness because they will eventually "forget" a wild measurement but in the process, it is possible that outliers can either cause the filter converge to an incorrect solution or worse become unstable. It would be interesting to compare a Kalman emitter location/tracking filter to a robust location/tracking formulation in the presence of mixed mode noise. A robust location/tracking formulation could be developed by simply applying a forgetting factor to older measurements in the robust update equations described in Chapter 4. Spingarn [Spi87] has compared extended and the extended iterated Kalman filter to batch least squares for normally distributed errors. Extending his work to include the just mentioned robust comparison would give a better understanding of existing Kalman location systems in the presence of outliers and may also reveal a valuable new robust approach for tracking moving emitters.

REFERENCES

[AU96] Air University. A Quick Look at Air Force 2025. Electronic document at *http://www.au.af.mil/au/2025/quicklk2.htm,* pages 1-4, December 1996.

[AY90] B. G. Agee and D. L. Young. Blind Capture and Geolocation of General Spatially Self-Coherent Waveforms Using Multiplatform SCORE. In *Conference Record of Twenty-Fourth Asilomar Conference on Signals, Systems and Computers*, pages 33-38, Pacific Grove, CA, November 1990.

[AD81] T.S. Arthanari and Y. Dodge. *Mathematical Programming in Statistics*. John Wiley & Sons, page 16, 1981.

[Bar97] R. S. Barr. Personal correspondence. Email, March, 1997.

[Boo82] S. A. Book. Least-Absolute-Deviations Position Finding. In *Naval Research Logistics Quarterly*, pages 235-246, June, 1982.

[BW84] J. B. Bednar and T. L. Watt. *Alpha-Trimmed Means and Their Relationship to Median Filters*. In IEEE Transactions on Acoustics, Speech, and Signal Processing, pages 145-153, February 1984.

[CS81] S. Chow and P. M. Schultheiss. Delay Estimation Using Narrow-Band Processes. In *IEEE Trans. Acoust., Speech, Signal Processing*, pages 478-484, June 1981.

[d'1893] M. d'Ocagne. Sur la determination geometrique du point le plus probable donne par un system de droites non convergentes. In *Journal de l'Ecole Polytechnique*, pages 1-25, Paris, 1893.

[EH69] H. Ekblom and S. Henriksson. Lp-Criteria for the Estimation of Location Parameters. In *SIAM Journal Applied Mathematics*, pages 1130-1141, Volume 17, 1969.

[Kri88] C. W. Kriel. *Lp Norm Estimation Techniques Applied to Multiple Emitter Location*. Ph.D. Thesis, Oklahoma State University, Stillwater, Oklahoma, 1988.

[KY88] C. W. Kriel and R. Yarlagadda. Lp Estimation Techniques Applied to Multiple Emitter Location. In *Proceedings of Forth Spectrum Estimation Conference,* pages 333-338, May 1988.

[MS84] H. Meyr and G. Spies. The Structure and Performance of Estimators for Real-Time Estimation of Randomly Varying Time Delay. In *IEEE Transactions on Acoustics, Speech, and Signal Processing*, pages 81-94, February 1984.

[Mar88] H. K. Mardia. Adaptive Multi-Dimensional Clustering for ESM. In *IEE Colloquium on Signal Processing for ESM Systems*, pages 40-45, Shipley, UK, April, 1988.

[USN97] United States Navy. Cost as An Indpendent Variable. In electronic form at *http://www.acq-ref.navy.mil/turbo/rfp14.htm*, April, 1997.

[Sch79] R. O. Schmidt. Multiple Emitter Location and Signal Parameter Estimation. In *Proceedings RADC Spectral Estimation Workshop*, pages 243-258, Rome, NY, 1979.

[Spi87] K. Spingarn. Passive Position Location Estimation Using the Extended Kalman Filter. In *IEEE Transactions on Aerospace and Electronic Systems*, pages 558-567, July, 1987.

[Sta47] R. G. Stansfield. Statistical Theory of D.F. Fixing. In *Journal Institute Electrical Engineering*, pages 762-770, volume 94, number 1, UK, 1947.

[Taf97] L. G. Taff. Target Localization From Bearings-Only Observations. In *IEEE Transactions on Aerospace and Electronic Systems*, pages 2-9, January 1997.

[Tah92] H. A. Taha. *Operations Research an Introduction.* Macmillan, page 164, fifth edition, 1992.

[Tor84] D. J. Torrieri. Statistical Theory of Passive Locations Systems. In *IEEE Transactions on Aerospace and Electronic Systems,* pages 183-198, March 1984.

[USA96] United States Air Force. *Air 2025*. Defense Technical Information Center, Ft. Belvior, VA, September 1996.

[WL90] E. Waltz and J. L Llinas. *Multisensor Data Fusion*. page 15, 1990, Artech House Inc., page 15, 1990.

[You96] D. L. Young. Linear Programming Solution for Bearings-Only Geolocation. Presented at the *Second Annual Southeast Conference on Linear Algebra*, College of William and Mary, Williamsburg, VA, March 1996.